

# We are IntechOpen, the world's leading publisher of Open Access books Built by scientists, for scientists

4,800

Open access books available

122,000

International authors and editors

135M

Downloads

Our authors are among the

154

Countries delivered to

TOP 1%

most cited scientists

12.2%

Contributors from top 500 universities



WEB OF SCIENCE™

Selection of our books indexed in the Book Citation Index  
in Web of Science™ Core Collection (BKCI)

Interested in publishing with us?  
Contact [book.department@intechopen.com](mailto:book.department@intechopen.com)

Numbers displayed above are based on latest data collected.  
For more information visit [www.intechopen.com](http://www.intechopen.com)



---

# **Review of Aerosol Observations by Lidar and Chemical Analysis in the State of São Paulo, Brazil**

---

Gerhard Held, Andrew G. Allen, Fabio J.S. Lopes, Ana Maria Gomes, Arnaldo A. Cardoso, Eduardo Landulfo

Additional information is available at the end of the chapter

<http://dx.doi.org/10.5772/50737>

---

## **1. Introduction**

Large-scale forest fires in the tropics, emitting vast amounts of aerosols and trace gases, drew the attention of scientists around the world in the late 80s and early 90s. A number of international collaborative research projects, such as TRACE-A (Transport and Atmospheric Chemistry near the Equator-Atlantic, [1]) and SAFARI-92 (South African Fire-Atmosphere Research Initiative, [2]), were initiated under the auspices of the International Geosphere-Biosphere Programme to investigate biomass burning emissions and their long-range transport. One of the areas of great interest was the Amazon region (Figure 1), which later led to the creation of the international Large Scale Biosphere-Atmosphere Experiment in Amazonia (LBA, [3]) in Brazil in 1998. Several intense observation campaigns were dedicated, not only to rainfall measurements by radar and storm structure, but also to biomass burning, monitoring of emissions and transport of aerosols and their impact on the vegetation and population of the region. However, monitoring of background concentrations of aerosols, deploying stacked filter units, had already been initiated in 1990 at the “Sierra do Navio” site (Amapá, about 190 km north of the equator) and in Cuiabá (Mato Grosso), a town located in the Brazilian savannah [4]. The location of both sites is shown in Figure 1.

São Paulo is Brazil’s most populous State, with approximately 42 million inhabitants (21,5% of Brazil’s total population) in an area of 249 000 km<sup>2</sup>. The region is diverse in terms of its geography, natural environment and economy, and can be broadly classified into three main zones. In the southeast, the Atlantic coastal strip is separated from the remainder of the State by the scarp of the Serra do Mar, containing Brazil’s largest remaining areas of

Atlantic rainforest, a threatened ecosystem that has been largely eliminated in most of the Brazilian States bordering the Atlantic ocean. Located on a plateau above the scarp are the densely populated and heavily industrialized regions of metropolitan São Paulo (RMSP) and its satellite cities. Continuing inland, the largest fraction of the area of the State has an economy mostly based on agro industry. Here has been widespread conversion of natural ecosystems to agriculture. The most important single agricultural activity is sugar cane production, although there are also substantial cattle ranching, citrus cultivation and agro forestry for pulping and construction. In all regions, it is largely local emission sources that determine the chemical composition of the atmospheric aerosol, with a smaller influence of long-range transport of polluted air masses from elsewhere in Brazil.



**Figure 1.** Brazil, showing the location of São Paulo State in relation to the Amazon region, as well as the background monitoring stations in Sierra do Navio (Amapá) and Cuiabá (Mato Grosso).

In terms of atmospheric quality, suspended aerosol particles are (together with ozone) probably the most important atmospheric pollutant in both São Paulo city and the largely agricultural hinterland of the State. Ozone is generated during reactions involving the nitrogen oxides ( $\text{NO}_x$ ) and volatile organic compounds (VOCs) emitted from vehicles, biomass burning and biogenic sources. The particulates are either emitted directly (in the form of primary aerosols), or are produced during reactions involving gaseous precursors ( $\text{SO}_2$ ,  $\text{NO}_x$  and hydrocarbons). In large urban areas, such as the Metropolitan Region of São Paulo (RMSP), anthropogenic emissions from vehicles and industrial processes are the dominant contributors to elevated aerosol levels, while biomass burning [5-7] and dust lifted from barren fields (Figure 2) during the dry winter season constitute the principal sources of aerosols in the central and western sectors of the state. The State of São Paulo is the largest producer of sugar cane in Brazil, accounting for about 60% of Brazil's harvest [8], with more than 4,7 million hectares planted in 2010, of which 44% are burnt before harvesting [9]. The sugar cane is mostly harvested from April to November. Although progress is being made in mechanization, large areas are still harvested manually, which

requires burning of the crop in sectors of the plantations during the night prior to manual cutting to remove excess foliage. This practice results in large quantities of aerosols and trace gases being emitted into the atmosphere (Figure 2a), not only negatively affecting local towns, but also regions much further downwind [10-12], demonstrating the importance of monitoring aerosols throughout the State.



(a)



(b)

**Figure 2.** (a) Typical sugar cane fire in central São Paulo State. (b) Dust lifted from freshly cut sugar cane fields by the downdraft of an approaching storm.

Along the São Paulo coast, marine aerosols are modified by the inclusion of pollutants emitted from transport, urban, and industrial sources. There are some areas where levels of anthropogenic pollution are low, and where the aerosol composition can be mainly attributed to natural origins. However, compared to metropolitan São Paulo and the interior of the State, the coastal zone has been much less well studied, with the exception of Cubatão, a heavily industrialized town near the coast close to Santos.

In the State of São Paulo, the first aerosol measurements began in Cubatão [13], and within the metropolitan area of São Paulo, notorious for its traffic emissions [14]. In terms of morphology, São Paulo is among the world's five largest cities, and is sixth largest in terms of population [15], with about 11,3 million inhabitants. The population of the Metropolitan Region of São Paulo (RMSP), which includes peripheral urban areas, reached an estimated 19,9 million persons in 2009 [16]. Human activities including road transport and industry now exert an enormous impact on air quality in the region, and therefore on the health of the population [17]. The total fleet of vehicles (cars, buses, trucks and motorcycles, powered by gasoline, ethanol and diesel) in the State of São Paulo exceeded 12,8 million in 2011, of which about 50% operate within the RMSP [9].

Observations from the Brazilian Lightning Detection Networks (RINDAT [18] and BrasilDAT at ELAT/INPE [19]) have shown a significantly higher lightning frequency over the RMSP and other large urban complexes within the State since the inception of the RINDAT Lightning Network in 1999 [20, 21]. This prompted a study of the impact of anthropogenic emissions on the frequency of lightning [22], showing a distinct increase of cloud-to-ground flashes, not only over the RMSP, but also over other large cities and densely populated or industrialized regions in the State, correlated to the occurrence of heat islands and increased concentrations of PM<sub>10</sub>.

## 2. Meteorology and climatology of the State of São Paulo

Since the meteorology of a region has a major impact on the dispersion or accumulation of pollutants, a brief characterization of the climate is appropriate. The State of São Paulo is located between the latitudes of about 20° and 25° South (Figure 1), thus falling into the transition zone from a tropical to a subtropical climate, with an annual rainfall total ranging between 1250 and 1650 mm in the interior, increasing to 1850 mm over the narrow coastal strip [23]. The year can be roughly divided into two periods, *viz.*, the rainy season from October to March, when most of the rain is produced by convective storms, and the dry winter months from April to September. During the rainy season, conditions are more representative of the tropical climate, with the occasional occurrence of a South Atlantic Convergence Zone (SACZ), which can be identified from satellite images as a cloud band with orientation northwest to southeast, extending from the southern region of Amazônia into the central region of the South Atlantic Ocean [24]. The SACZ situations can last more or less continuously from 4 days to more than one month and are extremely efficient producers of rain in the form of tropical thunderstorms, with accompanying high humidity. During the relatively dry winter months, the climatic conditions are more typical of the subtropics, with only occasional heavy rainfalls being caused by the passage of baroclinic systems (mostly cold fronts), moving from southwest to northeast across the State, but for the remaining time, the weather is dominated by a high pressure system, resulting in elevated temperatures, with low humidity and high stability in the Planetary Boundary Layer, favoring the accumulation of pollutants in the atmosphere of the region [25].

Sodar observations made during the period of June 2009 to December 2011 showed that strong nocturnal Low-Level-Jets (LLJs) develop on top of the surface radiation inversion, mostly during the relatively dry austral winter months (May – October), when stable conditions prevail [26, 27]. These LLJs generally form during the late evening at altitudes ranging from 250–500 m AGL, with maximum speeds of 12–20 m.s<sup>-1</sup>. They usually last until 08:00–09:00 Local Time (LT), when the inversion has been eroded by the solar radiation. The frequency of LLJs varied from 3 - 22 days per month, with higher frequencies and greater intensity generally during the winter months. Observations with a sodar were made at three different locations in the central region of the State, *viz.* in Bauru, Rio Claro and Ourinhos. Earlier measurements, deploying tethered balloons and radiosondes in the eastern region of the State, yielded similar results in terms of structure, dynamics, seasonality and development characteristics [28]. LLJs have been observed in many parts of the world and were found to have regional extent. The practical importance of the LLJ lies in the rapid transport of moisture and pollutants in a narrow vertical band above the radiation inversion [29].

### 3. Ground-level monitoring of particulates

Regular monitoring of air pollutants under the auspices of the Companhia de Tecnologia de Saneamento Ambiental (CETESB), the air quality “watchdog” in the State of São Paulo, started in the 70s, but a fully automatic monitoring network was only installed in 2000. Since then, observations are available in real time [30]. In 2001, 29 automatic stations, the majority in the RMSP, were already in operation [31]. From 2008 onwards, the automatic monitoring network was significantly expanded. In 2011, 42 monitoring stations in 28 towns were in operation, 19 in the RMSP and 23 in the remaining parts of the State [9]. The majority of the stations monitor particulate matter (PM<sub>10</sub>), NO, NO<sub>2</sub>, NO<sub>x</sub> and O<sub>3</sub>, as well as meteorological parameters, while a few also measure PM<sub>2.5</sub>, SO<sub>2</sub> and CO. The automatic air quality monitoring network is shown in Figure 3. Additionally, CETESB also maintained a network of 41 manual monitoring stations during 2011, where measurements are made of PM<sub>2.5</sub>, PM<sub>10</sub>, TSP (Total Suspended Particulates), black smoke and SO<sub>2</sub>, in various combinations [9]. Aerosol mass concentrations are determined using either  $\beta$ -attenuation instruments (automatic stations) or gravimetric and reflectometric techniques (manual stations).

In accordance with recommendations of the World Health Organization [32], CETESB defines 5 levels of air quality: “Boa” (good), “Regular” (regular), “Inadequada” (insufficient), “Má” (bad) and “Péssimo” (extremely bad), the highest being invoked if one of the monitored pollutants exceeds the pre-defined threshold. The national air quality standards are defined in CONAMA Resolution No. 03/90 (Table 2 in [9]).

PM<sub>10</sub> and TSP measurements are available since 1984 and 1985, respectively [31], although initially only from very few stations in the interior of the State, but gradually increasing to 41 and 11, respectively, in 2011 [9]. Figure 4 shows the year-to-year variation of annual mean PM<sub>10</sub> concentrations against the National Air Quality Standard (PQAr) for the RMSP and two sites in Cubatão (Figure 3, Nos. 24 and 25), which is one of the major industrial hubs in Brazil, where one site is located within the industrial suburb (No. 25) and the other in the

town centre (No. 24). A significant reduction of mean annual  $PM_{10}$  concentrations can be noticed from 1998 onwards, confirming the success of implementation of stringent air quality control measures, administered by CETESB. However, within the industrial suburb, confined in a valley, concentrations are still about twice the PQAr. A detailed description of Cubatão, its industrial activities and their location are found in [33]. More details on current  $PM_{10}$  and TSP concentrations are provided in Section 4.3.

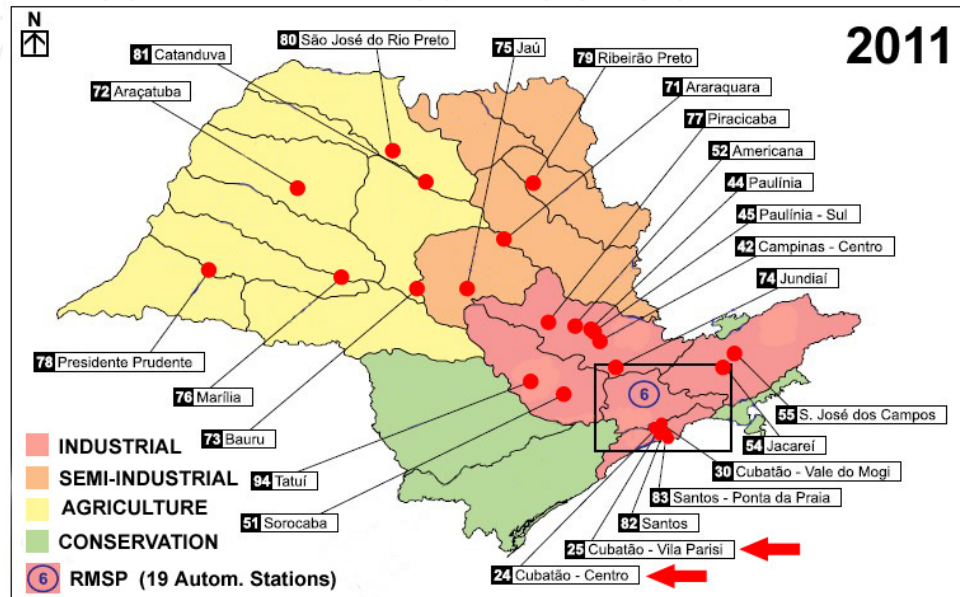


**Figure 3.** CETESB network of automatic monitoring stations in 2011. The shading indicates the principal land use in four schematic regions of the State, directly related to the type of emissions. Adapted from [9].

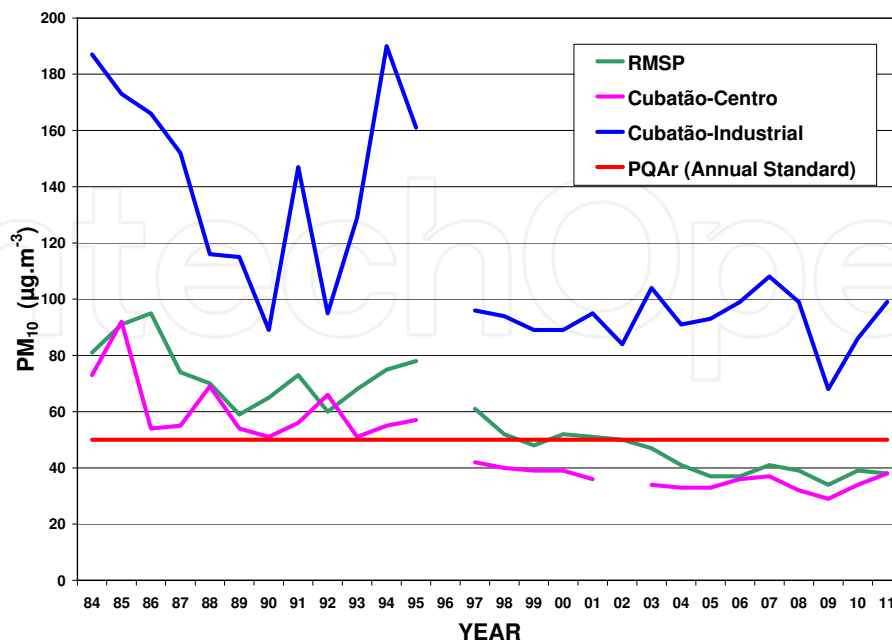


**Figure 4.** Year to year variation of  $PM_{10}$  from 1984 – 2011 for the RMSP and Cubatão. The data were extracted from [9, 31].  $PQAr = 50 \mu g.m^{-3}$  represents the Annual Standard.

Figure 5 demonstrates that the air quality in the interior of the State from 2002 to 2011, when a reasonable number of monitoring sites were already in operation [9], was generally well below the annual standard of  $50 \mu\text{g}\cdot\text{m}^{-3}$  for  $\text{PM}_{10}$ , with the exception of Santa Gertrudes, just south of Rio Claro (Figure 6), where several large ceramic industries are located, notorious for emitting large quantities of aerosols. At two other monitoring sites, annual means were close to the Annual Standard. At Limeira mixed industrial activities range from metallurgical, through cellulose to ceramics, besides sugar cane and orange production and processing plants. Limeira and Santa Gertrudes are medium-sized industrial towns, about 20 and 40 km northwest of Americana (Figure 3, No. 52). The other site is in Piracicaba (Figure 3, No. 77), which also hosts mixed industrial activities, including a significant petrochemical plant. However, the exceedance in 2011 was most likely caused by major road construction works in the immediate vicinity of the monitoring site [9].

Although annual mean concentrations of PM in the State of São Paulo seem to be quite acceptable, it is obvious that violations of the daily Air Quality Standard do occur occasionally in several towns of the interior and within the RMSP. Comprehensive annual and specialized technical reports and publications on the air quality in the State of São Paulo, including detailed monitoring results, are available online [9].

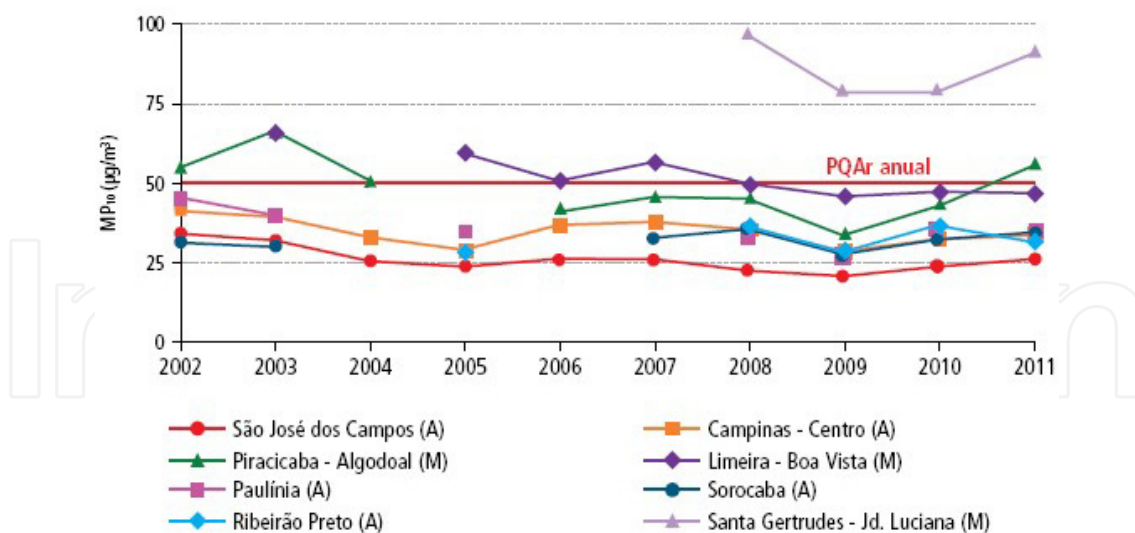


**Figure 5.** Year to year variation of  $\text{PM}_{10}$  from 2002 -2011 for monitoring sites in the interior of the State of São Paulo (after [9]).  $\text{PQAr} = 50 \mu\text{g}\cdot\text{m}^{-3}$  represents the Annual Standard.



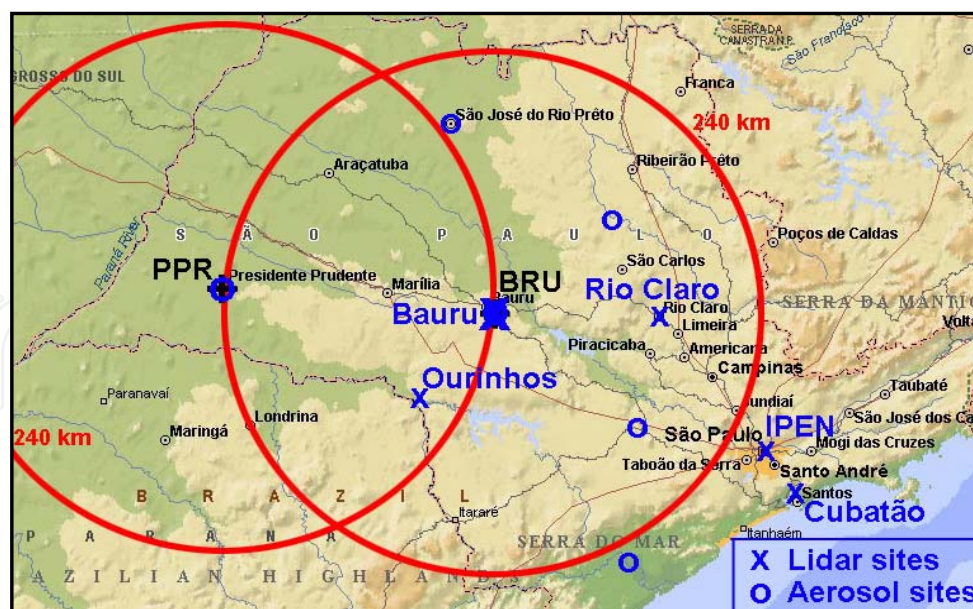


**Figure 6.** Aerosol monitoring sites in the State of São Paulo (except CETESB network) and 240 km ranges of IPMet's radars in Presidente Prudente (PPR) and Bauru (BRU). Sites from where lidar measurements are available are marked with x.

## 4. Chemical composition of aerosols

### 4.1. Agro-industrial rural regions

Seasonal variability in the major soluble ion composition of atmospheric particulate matter in the principal sugar cane growing region of central São Paulo State indicates that pre-harvest burning of sugar cane plants is an important influence on the regional-scale aerosol chemistry [34]. The size-distributed composition of ambient aerosols is used to explore seasonal differences in particle chemistry, and to show that dry deposition fluxes of soluble species, including important plant nutrients, increase during periods of biomass (sugar cane trash) burning [6, 10].

Concentrations of trace gases and aerosols were determined at six measurement sites of a regional network in São Paulo State (blue circles in Figure 6), installed in rural areas including the State's central agricultural zone and the eastern coast [11] as part of an experimental research project to determine the anthropogenic component of nutrient deposition. The measurements were made over 12 months during 2008/2009 (one week of continuous sampling per month). Aerosols were collected onto 47 mm diameter Teflon filters using active samplers, and trace gases ( $\text{NO}_2$ ,  $\text{NH}_3$ ,  $\text{HNO}_3$  and  $\text{SO}_2$ ) were sampled using diffusion-based devices. The soluble ions  $\text{NO}_3^-$ ,  $\text{NH}_4^+$ ,  $\text{PO}_4^{3-}$ ,  $\text{SO}_4^{2-}$ ,  $\text{Cl}^-$ ,  $\text{K}^+$ ,  $\text{Na}^+$ ,  $\text{Mg}^{2+}$  and  $\text{Ca}^{2+}$  were analyzed in aqueous extracts of the aerosol filters, using ion chromatography.  $\text{NO}_2$ ,  $\text{HNO}_3$  and  $\text{SO}_2$  were similarly determined as  $\text{NO}_2^-$ ,  $\text{NO}_3^-$  and  $\text{SO}_4^{2-}$ , following aqueous extraction of the collection media.  $\text{NH}_3$  was determined using a colorimetric technique. Identification and quantification of nutrient sources was achieved using principal component analysis (PCA) followed by multiple linear regression analysis (MLRA) applied

to the chemical data. Dry deposition fluxes were estimated using the measured atmospheric concentrations together with dry deposition velocities of gases and aerosols to different surface types, including tropical forest, savannah, sugar cane, pine, eucalyptus, orange, coffee, pasture and water. The annual cycle in deposition, to a sugar cane surface, of reactive nitrogen and sulphur in the gaseous, aerosol and dissolved phases is illustrated in Figure 7.

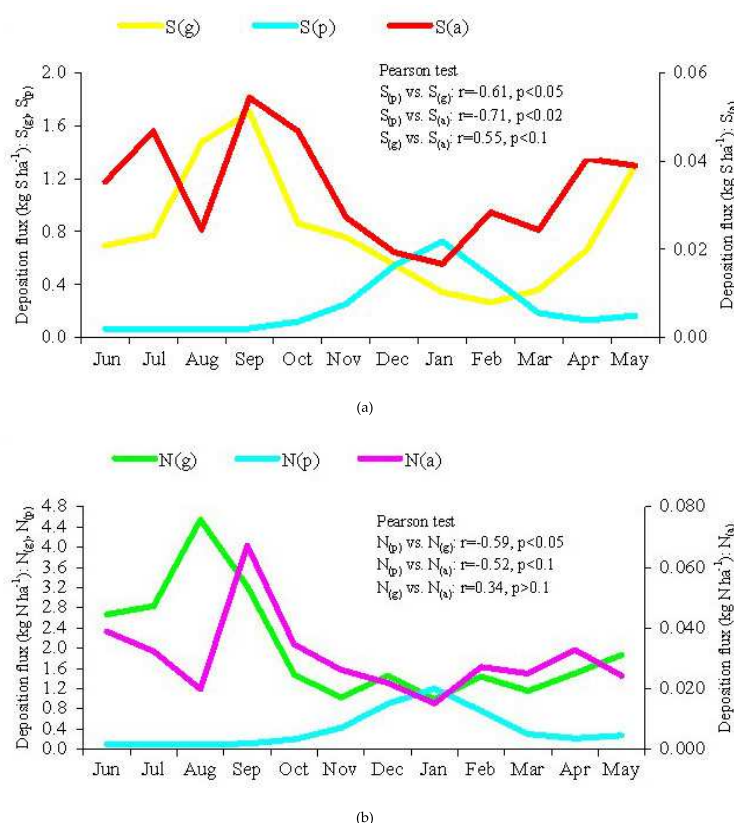


**Figure 7.** Annual cycle in deposition fluxes to a sugar cane surface of: **(a)** sulphur in gaseous ( $S(g)$ ), aerosol ( $S(a)$ ) and rainwater ( $S(p)$ ) phases; **(b)** nitrogen in gaseous ( $N(g)$ ), aerosol ( $N(a)$ ) and rainwater ( $N(p)$ ) phases. Primary y-axes: gas and rainwater; secondary y-axes: aerosol. Data for Araraquara.

The sugar cane industry has a major impact on air quality and the characteristics of the atmospheric aerosol. During the dry season (May to October), the burning of the cane, a prerequisite of manual harvesting, has for many years resulted in very large emissions of pollutants, including high carbon content aerosols. These particles contain water-soluble organic carbon (WSOC), anions (sulphates, nitrates and chlorides), cations (potassium, ammonium, calcium, magnesium, sodium), black carbon (BC), insoluble organic carbon and trace metals. Carbonaceous material comprises the bulk of the aerosol mass, especially in fine particles [5-7, 35-39]. In 2004, the annual emission of nitrogen oxides ( $NO_x$ ) from sugar cane burning in Sao Paulo State was in excess of 45 Gg.N [40]. This is not only indicative of the scale of the emissions, but also of their potential for formation of secondary aerosols (containing nitrates, amongst other components).

In 2011, annual mean  $PM_{10}$  concentrations measured at automatic monitoring stations in the agro-industrial interior of São Paulo State were in the range 23-91  $\mu\text{g}\cdot\text{m}^{-3}$ , with the highest

values at locations affected by primary emissions from ceramics industries (Figure 5). At sites in the sugar cane production areas, annual mean PM<sub>10</sub> concentrations were in the range of 32-41 µg.m<sup>-3</sup> [9]. The data revealed no obvious trends in PM<sub>10</sub> concentrations during the period 2002-2011 (Figure 5).

A proportion of the primary material emitted during sugar cane fires is in the form of the large ash fragments notorious for causing domestic soiling problems in the region. During 1995-1996, CETESB investigated deposition rates, and measured the concentrations of PAHs, PCBs, dioxins and furans. The sedimented material was collected during the harvest period using plastic funnels lined with polyurethane foam, positioned near to plantations and in the urban area of the city of Araraquara. Samples were also collected in parallel using a high volume filter-based sampler. Levels of PCBs were in the range 4-12 ng.m<sup>-3</sup>, and showed no association with levels of carbonaceous material derived from the fires. Deposition fluxes of the dioxins and furans were in the range 1-17 pg.m<sup>-2</sup>.day<sup>-1</sup>, and were higher in greater proximity to plantations, indicating that sugar cane burning was a source of these compounds. The PAHs were found in two distinct groups. Naphthalene, fluorene, phenanthrene, anthracene, fluoranthene, and pyrene were present at concentrations exceeding 30 ng.m<sup>-3</sup>, while acenaphthene, chrysene, benzo(a)fluoranthene, benzo(k)fluoranthene, benzo(a)pyrene, dibenzo(a,h)anthracene, benzo(g,h,i)perylene and indeno(1,2,3,c,d)pyrene were found at up to 21 ng.m<sup>-3</sup>. Concentrations were always higher during the harvest period [41].

The presence of PAHs in ash from sugar cane fires was also reported by Zamperlini *et al.* [42, 43]. In the PM<sub>10</sub> fraction, it was found that the most abundant polycyclic aromatic hydrocarbons were phenanthrene and fluoranthene, and the least abundant was anthracene [44]. Cluster analysis of the total PAH concentrations for each day of sampling, and the corresponding meteorological data, suggested that concentrations of PAHs were independent of climatological conditions or season of the year. Vehicular sources were identified during both dry and wet seasons, although sugar cane burning emissions were the dominant source during the dry season.

Sugar cane burning is a major source of acidic gases that contribute to the formation of secondary aerosols. In Araraquara, Da Rocha *et al.* [36] reported concentrations of 9,0 ppb (HCOOH), 1,3 ppb (CH<sub>3</sub>COOH), 4,9 ppb (SO<sub>2</sub>), 0,3 ppb (HCl) and 0,5 ppb (HNO<sub>3</sub>). Extremely high concentrations of these gases were measured in the plumes downwind of sugar cane fires: 1160-4230 ppb (HCOOH); 360-1750 ppb (CH<sub>3</sub>COOH); 10-630 ppb (SO<sub>2</sub>); 4-210 ppb (HCl); and 14-90 ppb (HNO<sub>3</sub>). Highest levels of SO<sub>2</sub>, HCl and HNO<sub>3</sub> in Araraquara were measured during the harvest period, with peak concentrations in the evening (the time of the fires).

The distribution of soluble ionic material between fine (<3,5 µm) and coarse (>3,5 µm) aerosol fractions was determined by Allen *et al.* [5], who measured the ions HCOO<sup>-</sup>, CH<sub>3</sub>COO<sup>-</sup>, C<sub>2</sub>O<sub>4</sub><sup>2-</sup>, SO<sub>4</sub><sup>2-</sup>, NO<sub>3</sub><sup>-</sup>, Cl<sup>-</sup>, Na<sup>+</sup>, K<sup>+</sup>, NH<sub>4</sub><sup>+</sup>, Mg<sup>2+</sup> and Ca<sup>2+</sup>. The fine and coarse particles showed acidic and basic properties, respectively, and concentrations of all major ions increased significantly during the dry season (Figure 8). Da Rocha *et al.* [6] collected aerosols

in twelve size fractions, and used calculation of ion equivalent balances to show that during burning periods, the smaller particles (Aitken and accumulation modes) were more acidic, containing higher concentrations of  $\text{SO}_4^{2-}$ ,  $\text{C}_2\text{O}_4^{2-}$ ,  $\text{NO}_3^-$ ,  $\text{HCOO}^-$ ,  $\text{CH}_3\text{COO}^-$  and  $\text{Cl}^-$ , but insufficient  $\text{NH}_4^+$  and  $\text{K}^+$  to achieve neutrality. Larger particles showed an anion deficit due to the presence of unmeasured ions, and comprised re-suspended dusts modified by accumulation of nitrate, chloride and organic anions. Increases of re-suspended particles during the burning season were attributed to release of earlier deposits from the surfaces of burning vegetation, as well as increased vehicle movement on unsealed roads. During the winter months, the relative contribution of combined emissions from road transport and industry diminished due to increased emissions from biomass combustion and other activities specifically associated with the harvest period.

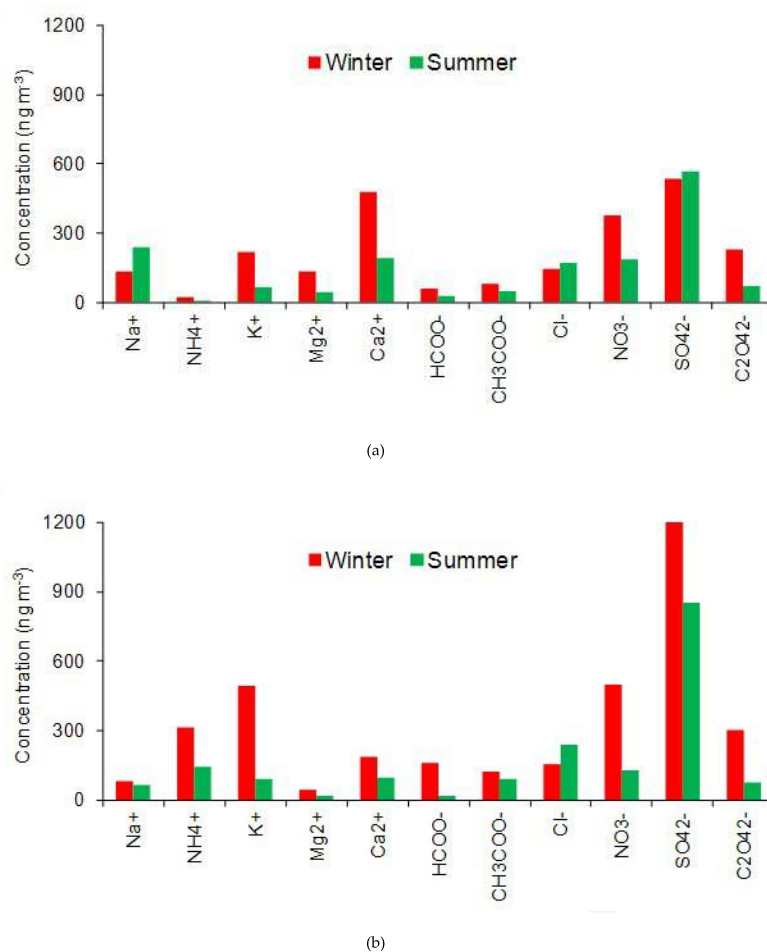


**Figure 8.** Comparison of aerosol composition in the Araraquara region during winter (biomass burning) and summer (non-burning) periods: **(a)** Coarse particles; **(b)** fine particles.

In separate work, biomass-burning aerosols were found to contribute around 60 and 25% of the mass of fine and coarse aerosols, respectively, in the Piracicaba sugar cane growing region [7]. A high proportion of the elements K, S, Cl, Br, Fe and Si in aerosols has been linked to biomass burning [45], indicative of both a combustion component (emissions of K, S, Cl and Br) and a suspended soil dust component (emissions of Fe and Si).

In a study reported in [38], elemental analysis of individual and bulk aerosols collected in rural areas was followed by evaluation of the data using statistical hierarchical clustering, which revealed the contributions of two different types of carbonaceous material (biogenic and carbon-rich) and two aluminosilicate fractions (pure or mixed with carbon). These findings contrasted with the findings of similar work in the atmosphere of São Paulo city, where hierarchical clustering analysis revealed the presence of metal compounds, silicon-rich particles, sulphates, carbonates, chlorides, organics and biogenic particles [46]. This reflects the very different characteristics of the aerosols found in the two regions.

Da Rocha *et al.* [6] showed that dry deposition fluxes of important plant nutrients increased during the sugar cane burning season. During this period, the fine fraction aerosol was more acidic and contained elevated concentrations of  $\text{SO}_4^{2-}$ ,  $\text{C}_2\text{O}_4^{2-}$ ,  $\text{NO}_3^-$ ,  $\text{HCOO}^-$ ,  $\text{CH}_3\text{COO}^-$  and  $\text{Cl}^-$ , but insufficient  $\text{NH}_4^+$  and  $\text{K}^+$  to achieve neutrality. Larger particles consisted of re-suspended dust, modified by inclusion of nitrate, chloride and organic anions. The increases in annual particulate dry deposition fluxes due to higher fluxes during the sugar cane harvest were 44,3% ( $\text{NH}_4^+$ ), 42,1% ( $\text{K}^+$ ), 31,8% ( $\text{Mg}^{2+}$ ), 30,4% ( $\text{HCOO}^-$ ), 12,8% ( $\text{Cl}^-$ ), 6,6% ( $\text{CH}_3\text{COO}^-$ ), 5,2% ( $\text{Ca}^{2+}$ ), 3,8% ( $\text{SO}_4^{2-}$ ) and 2,3% ( $\text{NO}_3^-$ ). The contributions of dry deposition to total deposition (including precipitation scavenging, excluding gaseous dry deposition) were 31% ( $\text{Na}^+$ ), 8% ( $\text{NH}_4^+$ ), 26% ( $\text{K}^+$ ), 63% ( $\text{Mg}^{2+}$ ), 66% ( $\text{Ca}^{2+}$ ), 32% ( $\text{Cl}^-$ ), 33% ( $\text{NO}_3^-$ ) and 36% ( $\text{SO}_4^{2-}$ ).

Deposition rates of aerosol nutrient species to a range of natural and agricultural surfaces were reported in [10], using a size-segregated particle dry deposition model. Fluxes greatly exceeded those expected under pristine conditions, with deposition to tropical forest found to have increased by factors of 12,2 ( $\text{NO}_3^-$ ), 6,2 ( $\text{PO}_4^{3-}$ ) and 2,6 ( $\text{K}^+$ ) (Figure 9). Source apportionment using principal component analysis (PCA) and multiple linear regression analysis (MLRA) revealed that in central São Paulo State, biomass burning, products of secondary reactions and soil dust re-suspension contributed 43%, 31% and 21% of  $\text{PM}_{2.5}$  mass, respectively. Re-suspension and biomass burning contributed 22% and 19%, respectively, to  $\text{PM}_{10}$  mass, and re-suspension accounted for approximately half the mass of coarse particles. At least 40% of  $\text{NO}_3^-$ -N, 20% of phosphorus and 55% of potassium deposited originated from agriculture-related emissions.

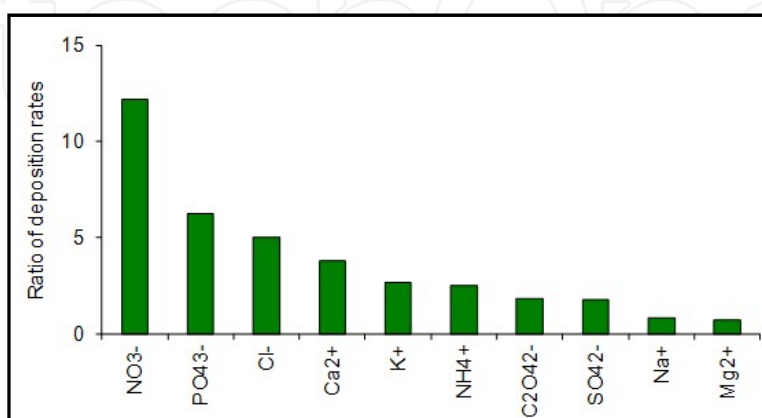


**Figure 9.** Graph showing the present-day increase in aerosol dry deposition rates to a tropical forest surface, compared to deposition rates estimated for pristine conditions.

Emissions of reactive nitrogen compounds are of concern due to their influence on both atmospheric acidity (production of  $\text{HNO}_3$  from reactions involving  $\text{NO}_2$ ) and the formation of photochemical oxidants such as ozone and peroxyacetyl nitrate (PAN). Reactions of acidic species with ammonia generate ammonium sulphates and nitrates, mainly in the long-lived accumulation mode size fraction. Deposition of reactive nitrogen can cause eutrophication of water bodies, as well as the release of trace metals in soils. Machado *et al.* [47] found that emissions of reactive nitrogen during sugar cane burning, in the forms of  $\text{NH}_3$ ,  $\text{NO}_x$  and particulate nitrate and ammonium, were equivalent to 35% of the annual fertilizer-N application. The concentrations of nitrogen oxides showed a positive association with the number of fires, reflecting the importance of biomass burning as a major emission source, and mean concentrations of  $\text{NO}_x$  in the dry season were twice those in the wet season. During the dry season, biomass burning was the main source of  $\text{NH}_3$ , with other sources (wastes, soil, biogenic) predominant during the wet season. The estimated emission fluxes of  $\text{NO}_2\text{-N}$ ,  $\text{NH}_3\text{-N}$ ,  $\text{NO}_3\text{-N}$  and  $\text{NH}_4^+\text{-N}$  from sugar cane burning in a planted area of about  $2,2 \times 10^6$  ha were 11,0, 1,1, 0,2 and 1,2  $\text{Gg.N.yr}^{-1}$ , respectively.

The sources, atmospheric transport and reactions of the main inorganic reactive nitrogen ( $\text{N}_r$ ) species ( $\text{NO}_2$ ,  $\text{NH}_3$ ,  $\text{HNO}_3$  and aerosol nitrate and ammonium) were investigated in a study conducted over a period of one year at six sites distributed across an area of about 130,000  $\text{km}^2$  in São Paulo State [11]. Oxidized forms of nitrogen were estimated to account for about 90% of dry deposited  $\text{N}_r$ , due to the emissions of nitrogen oxides from biomass burning and road transport.  $\text{NO}_2\text{-N}$  was important closer to urban areas; however,  $\text{HNO}_3\text{-N}$  was the largest individual component of dry deposited  $\text{N}_r$ . A simple mathematical model was developed to enable determination of total  $\text{N}_r$  dry deposition from knowledge of  $\text{NO}_2$  concentrations. The model, whose error ranged from <1% to 29%, provided a new tool for the mapping of reactive nitrogen deposition.

The sugar cane burning emissions radically alter the chemistry of precipitation water. Coelho *et al.* [122] found that concentrations of soluble ions ( $\text{K}^+$ ,  $\text{Na}^+$ ,  $\text{NH}_4^+$ ,  $\text{Ca}^{2+}$ ,  $\text{Mg}^{2+}$ ,  $\text{Cl}^-$ ,  $\text{NO}_3^-$ ,  $\text{SO}_4^{2-}$ ,  $\text{F}^-$ ,  $\text{PO}_4^{3-}$ ,  $\text{CH}_3\text{COO}^-$ ,  $\text{HCOO}^-$ ,  $\text{C}_2\text{O}_4^{2-}$  and  $\text{HCO}_3^-$ ) increased by between two and six-fold during the harvest period. Principal component analysis revealed three main sources of the material in rainwater: biomass burning and soil dust re-suspension (52% of the total variance), secondary aerosols (26%) and vehicular emissions (10%). The biomass burning component diminished in the summer (non-burning period), when there was a relative increase in the importance of road transport/industrial emissions. The volume-weighted mean concentrations of ammonium ( $23,4 \mu\text{mol.L}^{-1}$ ) and nitrate ( $17,5 \mu\text{mol.L}^{-1}$ ) in rainwater samples collected during the harvest period were similar to those found in rainwater from São Paulo city, which emphasized the importance of including rural agro-industrial emissions in regional-scale atmospheric chemistry and transport models. There was evidence of a biomass-burning source throughout the year, which suggests that vegetation fires may continue to emit aerosols and their precursor gases, even after sugar cane burning is phased out.

## 4.2. Metropolitan São Paulo (RMSP)

In terms of trace species, the composition of the lower troposphere in the conurbation of the RMSP differs considerably from that of the interior of the State and the coastal zone. The critical air quality issue here is the scale of the emissions from road vehicles. In 2001, the vehicle fleet consisted of 17,2% hydrated ethanol-fuelled, 76,3% gasohol-fuelled and 6,5% diesel-fuelled vehicles, with ethanol contributing 34% of the total fuel consumption [31]. The figures for 2011 were 46,7% gasohol (cars and light commercial), 3,9% hydrated ethanol, 31,9% flex-fuel, 5,4% diesel and 12% motorcycles [9].

It is important to consider the relative amounts of the different fuels used, since emissions vary according to fuel, which has consequences for aerosol composition. For example, there is a larger fraction of oxygenated compounds in the secondary aerosols produced from reactions involving the aldehydes and alcohols emitted during ethanol combustion, which can affect the hygroscopicity of the particles, as well as their toxicological properties [48, 49].

The proportions of gasohol (gasoline with 22% anhydrous ethanol) and hydrated ethanol used have varied considerably in recent decades. Ethanol was first adopted as a road vehicle fuel in Brazil in 1979, due to the Brazilian National Alcohol Program (PROALCOOL), which was introduced as a response to the 1970s oil crisis. This not only reduced Brazil's dependency on oil imports, but also helped to eliminate the use of lead-containing anti-knock additives [49]. Sales of hydrated ethanol-fuelled vehicles peaked in the 1980s [50]. More recently, since around 2005, the new car market has been dominated by flex-fuel vehicles equipped with engine systems able to adjust to the gasoline/ethanol mixture present in the fuel tank [9].

In 2011, the sources of PM<sub>10</sub> in metropolitan São Paulo were: heavy goods vehicles (38,6%), re-suspended dusts (25%), secondary aerosols (25%), industrial processes (10%) and light duty vehicles (1,4%). Annual mean concentrations of PM<sub>10</sub> measured at the 18 automatic monitoring stations in São Paulo ranged between 31 and 50  $\mu\text{g}\cdot\text{m}^{-3}$  [9]. A detailed analysis of these measurements, as well as of PM<sub>2.5</sub>, TSP and black smoke measurements made at a smaller number of locations, are provided in the CETESB report [9] and in earlier annual reports published by CETESB.

The pollutant source profile remains fairly constant throughout the year. Use of absolute principal factor analysis showed that the contributions of different sources to PM<sub>2.5</sub> mass during winter and summer were: vehicle emissions (28 and 24% for the two seasons, respectively), re-suspended soil dusts (25 and 39%), oil combustion (18 and 21%), sulphates (23 and 17%) and industrial emissions (5 and 6%). Soil dusts accounted for 75-78% of the mass of coarse particles [51]. Andrade *et al.* [14] reported the results of elemental analyses, using particle-induced X-ray emission (PIXE) analysis of fine and coarse aerosols collected in 1989. Principal component analysis revealed the following sources of fine particles: oil and diesel combustion (explaining 41% of the mass), re-suspended soil dusts (18%), industrial emissions (13%), and a source associated with emissions of Cu and Mg (18%). Sources of coarse particles were: re-suspended soil dusts (59%), industrial emissions (19%),

oil burning (8%) and marine aerosols (14%). Alonso *et al.* [52] used chemical mass balance (CMB) receptor modeling to show that the composition of fine particles was consistent with the presence of primary material from vehicles and secondary organic carbon and sulphate. Road dust re-suspension and vehicle emissions were the main sources of coarse particles and TSP. The same trends in source profiles were observed at geographically distinct locations in São Paulo. Sanchez-Ccoyllo and Andrade [53] used receptor modeling to identify five main sources of aerosols: vehicles, waste incineration, vegetation, suspended soil dust and fuel oil burning.

Organic and elemental carbon, emitted mainly from diesel vehicles, together with ammonium sulphate, make up most of the mass of fine particles [54, 55]. In [56] it is reported that 80% of the mass of fine (PM<sub>2.5</sub>) particles consisted of organic material, with SO<sub>4</sub><sup>2-</sup>, NO<sub>3</sub><sup>-</sup> and NH<sub>4</sub><sup>+</sup> present in the fine fraction, and NO<sub>3</sub><sup>-</sup>, SO<sub>4</sub><sup>2-</sup>, Ca<sup>2+</sup>, and Cl<sup>-</sup> predominant in coarse particles (PM<sub>2.5-10</sub>). Albuquerque *et al.* [57] found that fine particles were rich in BC, S and Pb, while elements associated with crustal aerosols and/or industrial emissions (Al, Si, Ca, Ti, and Fe), together with ammonium sulphate and BC, composed the coarse mode particles. Other species, including K, Al, Fe and soil minerals, are included as a smaller component of fine particle mass [46]. Both vehicular and industrial emissions are sources of trace metals (Zn, Pb, Cr, Mn, Cd, etc.) [58, 59], and there appear to be continuing emissions of Pb from the road vehicle fleet, despite apparently low levels of Pb in fuels [60].

Aerosol composition similar to that of São Paulo is found in other major conurbations. In Campinas, the second largest city in the State, 100 km inland from São Paulo, fine particles were found to consist of 48% elemental carbon and 22% organic carbon, together with soluble ions and trace elements [61].

The PM concentrations are influenced not only by the magnitudes of emission sources, but also by ventilation and relative humidity. Miranda and Andrade [54] reported that higher PM<sub>10</sub> concentrations (105 µg.m<sup>-3</sup>) measured during the winter of 1999, compared to winter 2000 (60 µg.m<sup>-3</sup>), were due to both better ventilation of the city during the latter period, as well as an increase in particle sizes at higher humidity. Similar findings were reported in [53], with lower pollutant levels associated with increased ventilation, precipitation, and relative humidity.

Primary emissions from vehicles result in large diurnal cycles in the concentrations of PM<sub>10</sub>, BC, CO, NO<sub>x</sub> and SO<sub>2</sub> [51], however the diurnal trends in particle mass concentrations differ between highly polluted and less polluted periods, with concentrations higher during the daytime for the former, and during the nighttime for the latter [57]. A possible influence of humidity on both the mass and size distribution of the Sao Paulo aerosol was suggested by the observation that while the size distribution of ammonium sulphate was unimodal during the daytime (with a maximum at 0,38 µm), at night, when humidity is higher, the size distribution was bimodal (with maxima at 0,38 and 0,59 µm) [55]. Furthermore, particle growth, observed using a Scanning Mobility Particle Sizer (SMPS), has been found to increase under polluted conditions [57].



Although local sources are by far the most important contributors to particulate air pollution in São Paulo city, back-trajectory analysis has shown that the atmosphere of the city can also be affected by the advection of air masses from distant regions where agricultural biomass burning is practiced, especially northeast Brazil [62]. This could explain the finding that the relative contribution of ammonium sulphate is higher under less polluted conditions [57].

An important consequence of the prevalence of fine mode particles in the atmosphere of the city is that the indoor environment provides little or no protection against exposure to these pollutants, since they easily infiltrate buildings. This was observed [63] using simultaneous indoor and outdoor measurements of a range of ionic species associated with both primary emissions (potassium, magnesium, sodium and calcium) and secondary aerosol formation (chloride, acetate, nitrate, formate, pyruvate, nitrite, sulphate, oxalate and ammonium). The measurements were made in offices, restaurants and a hotel. In the fine mode, only oxalate and ammonium showed significantly lower concentrations indoors. In the coarse mode, lower concentrations were normally found indoors (with the exception of acetate, chloride and potassium), reflecting the less efficient infiltration of larger aerosols.

Polycyclic aromatic hydrocarbons are an important component of the urban aerosols. Chrysene, benzo(e)pyrene and benzo(b)fluoranthene were found to be the predominant PAHs in  $PM_{10}$ , originating from industry, vehicles and long-range transport [64]. Levels of  $PM_{10}$  similar to those in São Paulo were measured in a city (Araraquara) situated in the rural biomass burning zone, although here PAH concentrations were lower. In both cases, dry deposition appeared to be the main mechanism of removal of PAH-containing aerosols from the atmosphere [65].

Bourotte *et al.* [66] measured the concentrations of 13 PAHs in fine ( $PM_{2.5}$ ) and coarse ( $PM_{2.5-10}$ ) aerosols. In both fractions, the predominant compounds were indeno(1,2,3-cd)pyrene, benzo(ghi)perylene and benzo(b)fluoranthene and PAH ratios suggested that automobile exhaust was the main source of the compounds. Factor analysis revealed four source components for the  $PM_{2.5}$  fraction: diesel emissions, stationary combustion, vehicle emissions, and combustion of natural gas and biomass. For the coarse fraction, two components were identified, corresponding to vehicles and a mixture of gas, oil, and waste combustion.

### 4.3. Coastal regions

Although measurements of atmospheric aerosol are scarce in most of the coastal regions, an exception is the industrialized town of Cubatão, located near sea level at the base of the Serra do Mar scarp, where there is a large industrial complex comprising over 20 heavy industries (petrochemical, chemical, iron and steel, fertilizer, cement, coking and others). The monitoring stations in this area register regular episodes of particulate pollution, with the emissions from the industrial installations being entrained into a sea breeze circulation, when  $PM_{10}$  concentrations can increase by as much as an order of magnitude [67]. Pollutants absorbed into cloud water and precipitation are subsequently deposited to the vegetation of the Serra do Mar Atlantic rainforest, causing extensive ecological damage [68].

Due to extreme levels of pollution, air quality in the Cubatão region has been monitored by CETESB since the 1980s, and there are currently three sites where PM<sub>10</sub> is continuously measured (Figure 5), and one where TSP is measured [9]. The case of Cubatão is unique, since in contrast to the RMSP, by far the largest source of particulates is industrial emissions, rather than road transport. Guideline levels of TSP and PM<sub>10</sub> have been frequently exceeded in the industrial zone (Vila Parisi) of Cubatão, and there has been no improvement in PM<sub>10</sub> levels in recent years. During 2011, the annual mean PM<sub>10</sub> concentrations in the three zones of Cubatão were 99 µg.m<sup>-3</sup> (Vila Parisi), 61 µg.m<sup>-3</sup> (Vila Mogi) and 38 µg.m<sup>-3</sup> (Centro) [9]. At the industrial Vila Parisi site, the annual geometric mean TSP concentration was 236 µg.m<sup>-3</sup>, greatly exceeding the primary and secondary air quality standards for this pollutant species (80 and 60 µg.m<sup>-3</sup>, respectively).

Although industrial emissions are responsible for the largest proportion of the aerosol loading of the atmosphere near the Cubatão industrial complex, the organic fraction has an important road transport-related component, because concentrations of polycyclic aromatic hydrocarbons (PAHs) are governed by emissions from heavy duty diesel vehicles [69]. In the same work, it was reported that a shift to greater use of biodiesel might decrease emissions of the PAHs.

In regions distant from the industrial installations, the aerosol composition reflects mainly natural sources (biogenic, terrigenous and marine). Bourotte *et al.* [70] found that aerosol (PM<sub>10</sub>) composition in a State Park in the Cunha region was characterized by an abundance of K<sup>+</sup>, Ca<sup>2+</sup>, Na<sup>+</sup>, Cl<sup>-</sup> and Pb, while Vasconcellos *et al.* [71] reported the presence of aliphatic hydrocarbons emitted from biogenic sources in the coastal region.

## 5. Lidar observations

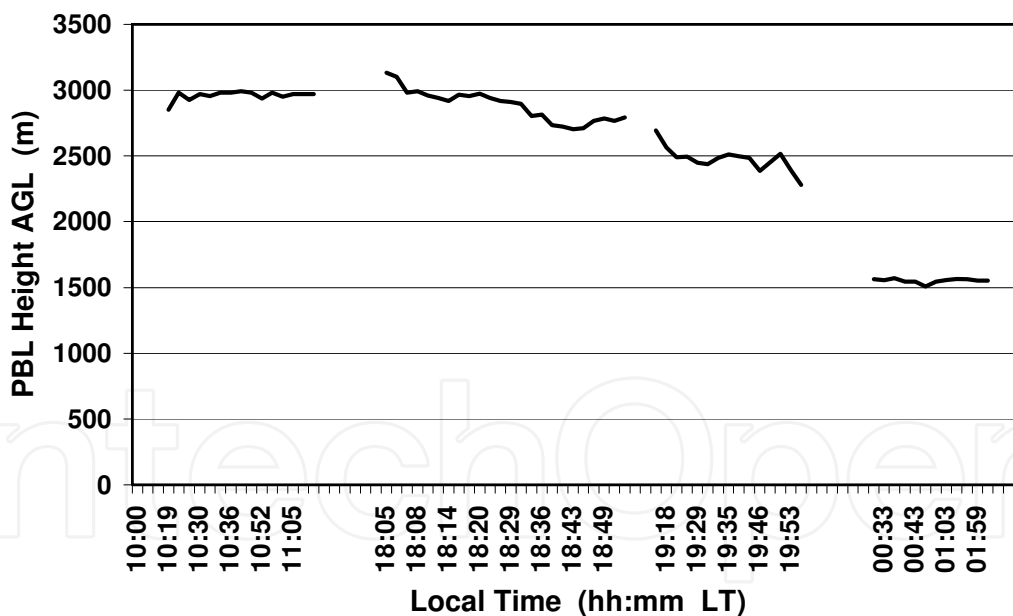
### 5.1. MSP-Lidar

In 2001, an elastic backscattering lidar system (MSP-Lidar) was installed in a suburban area of São Paulo city, on the Campus of the University of São Paulo (23°33' S, 46°44' W; Figure 6) and is being operated by the *Centro de Lasers e Aplicações* (CLA) of the *Instituto de Pesquisas Energéticas e Nucleares* (IPEN). The lidar is collocated with an AERONET sunphotometer, which provides the vertical profile of the aerosol backscatter coefficient at 532 nm up to an altitude of 4–6 km above sea level [72]. The MSP-Lidar comprises a Nd:YAG laser with a wavelength of 532 nm, and is operated with a repetition rate (PRF) of 20 Hz and an energy pulse of up to 120 mJ. The backscattering signal is captured by a Newtonian telescope with 1.5 m focal length. Attached to the telescope is a photomultiplier optimized for the visible spectrum with a 1 nm FWHM interference filter. Observations are being made whenever atmospheric conditions (absence of low or middle clouds; no rain) permit the operation of the lidar, resulting in a vast amount of data having been accumulated, which have so far been exploited in 5 MSc and 4 PhD theses, the most relevant being [73-76].

In January 2004, the IPEN MSP-Lidar system was installed for 6 weeks at IPMet in Bauru (Figure 6), located in the central part of São Paulo State, to provide the first measurements of

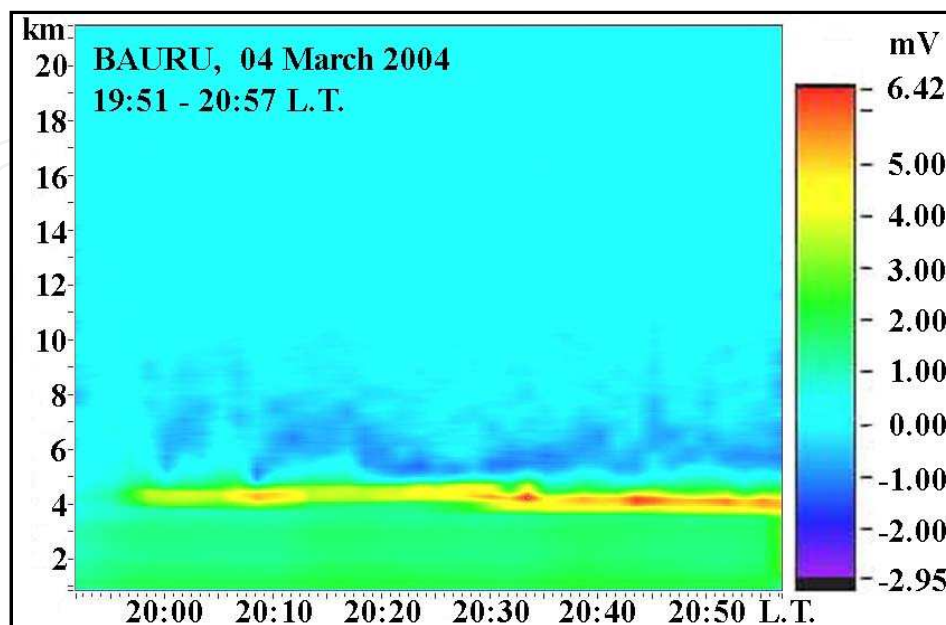
aerosol layers in the interior of the State [77]. At the beginning of the campaign, the lidar was operated in its original configuration and the data were digitized using a digital oscilloscope with 1 GHz bandwidth and 11-bit resolution; at the end of January 2004, this device was replaced by a transient recorder, capable of simultaneous analog and photon counting measurements at higher resolution (12-bit). The system was operated on 31 different days, during periods of about 4 hours in the morning, 4 hours in the afternoon and 6-8 hours during the night, depending on the occurrence of cloud and/or precipitation. The daytime measurements had a 15-30 m spatial resolution and maximum altitude of 10 km, yielding information on the diurnal variation of the Planetary Boundary Layer (PBL), while the measurements at night had a 30-60 m resolution, reaching up to 30-35 km maximum altitude. The diurnal variation of the PBL during the austral summer could be documented, as well as some background concentrations of aerosols, because very little biomass burning takes place during the rainy period.

Figure 10 shows a typical example of the diurnal variation of the height of the PBL on a cloudless day in Bauru. It should be noted that, due to the latitude of  $-22,3^\circ$ , the lidar cannot be operated during the midday period in summer, but as a result of turbulent mixing, the PBL could easily reach a maximum height of  $\geq 3,5$  km above ground level (AGL) during the early afternoon. The top of the PBL starts decreasing well before sunset, until it stabilizes at around 1,5 km AGL during the night. Times are indicated in Local Time (LT = UT-3h).



**Figure 10.** Height of the PBL over Bauru on 01/02 March 2004 for four different periods (10:19-11:08; 18:05-18:55; 19:13-19:54; 00:27-02:02 LT), with a vertical resolution of 30 m (after [78]).

The increased vertical range of the lidar during nocturnal operation permitted the detection of thin clouds and layers of aerosols, as shown in Figure 11. A cloud layer is clearly visible at around 4,5 km, while aerosols were detected at 3 and 5 km AGL, respectively. The top of the PBL is at about 1850 m AGL, with the faint layering being indicated in shades of green and light-blue colours.



**Figure 11.** Nocturnal lidar observation above Bauru on 04 March 2004. Vertical range from 855 m to 21,5 km AGL, with a resolution of 30 m (after [78]).

In early 2008, the MSP-Lidar system was upgraded to a Raman lidar, and in its present 3-channel configuration it can measure elastic backscatter at 355 nm, together with nitrogen and water vapour Raman backscatters at 387 nm and 408 nm, respectively. Therefore, the PBL data now available include aerosol backscattering and extinction coefficients, as well as the Lidar Ratio (LR) and water vapour mixing ratio. Figures 12 and 13 present typical results of Raman lidar measurements recorded during night-time of 09/10 January 2008, during the austral summer season. This period of the year is characterized by a very well defined boundary layer throughout the day and relatively high humidity. The major part of aerosols and water vapour is contained within the boundary layer, while the scattering above the PBL is mainly due to molecules. Figure 12 shows the aerosol extinction and backscattering coefficient profiles at 355 nm, where one can see a residual aerosol layer between 900 m and 2000 m AGL, indicating a very pronounced presence of aerosols, overlaid by another discrete layer above it between 2500 m and 3500 m AGL. The height profile of the Lidar Ratio is shown in Figure 13a. The Lidar Ratio is about 80 sr and stable throughout the PBL up to about 3000 m AGL. The vertical profile of the lidar-derived water vapour mixing ratio can be seen in Figure 13b. The calibration of the lidar was performed using radiosonde data from the nearby São Paulo Campo de Marte airport. Although the sonde had a relatively low height resolution, integrating the water vapour content with height made such calibration possible.

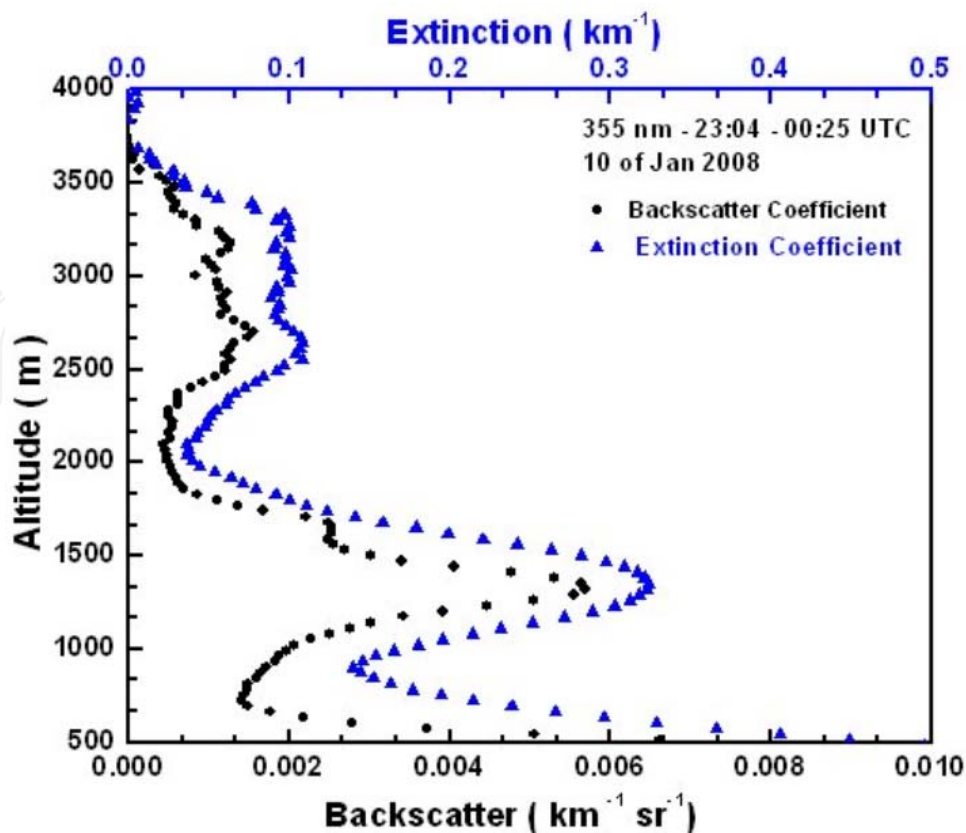
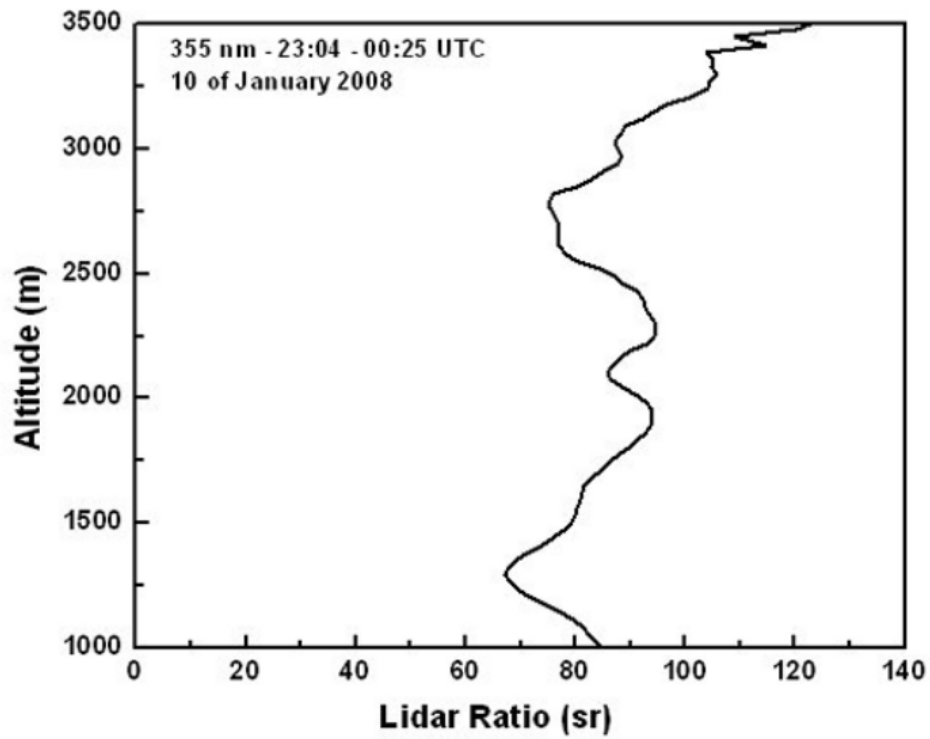


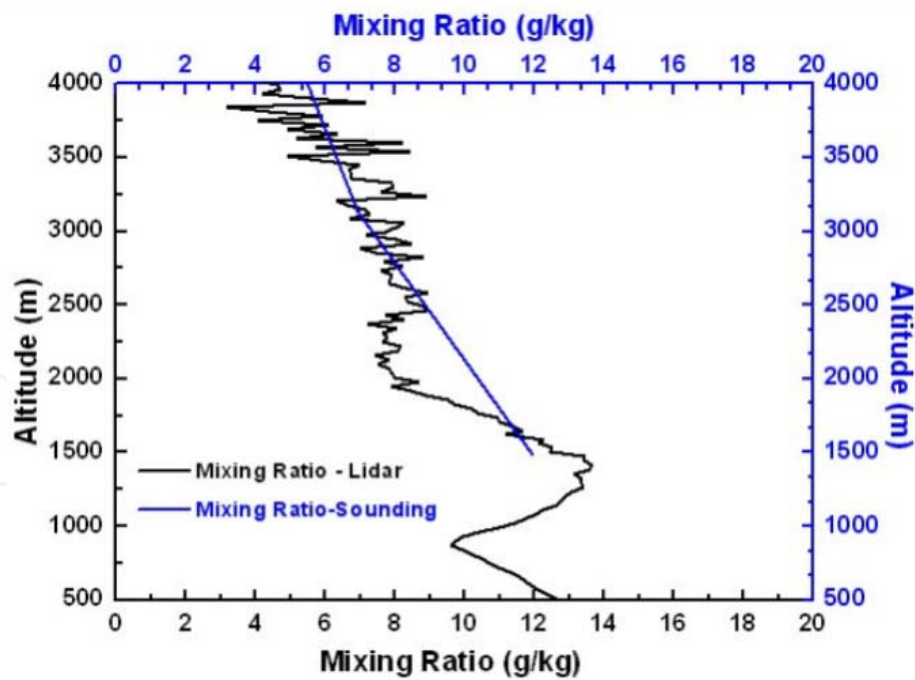
**Figure 12.** Aerosol backscatter and extinction profiles at 355 nm observed on 10 January 2008 at 00:25 UT (21:25 LT). The PBL top height is considered to be at 2000 m.

The MSP-Lidar system has contributed to several studies concerning the properties of aerosols and their influence on the air quality index of the city of São Paulo. Lidar measurements conducted daily provided observations of the PBL variation, which could be compared to corresponding air quality index values from local air quality monitoring and management agencies, as well as identifying potential air dispersion conditions [79]. It has also been deployed to monitor the long-range transport of aerosol plumes from different regions of Brazil to the RMSP and to evaluate the contribution of aerosol pollutants from remote sources. Landulfo and Lopes [80] have analyzed an event during the period 02 - 09 August 2007 when the AOD (Aerosol Optical Depth) and AE (Ångström Exponent) values retrieved from the AERONET sunphotometer indicated that high aerosol loads at five different locations in the Brazilian territory corresponded to biomass-burning particles. This was validated by the mean values of the Total Attenuated Backscatter Coefficient at 532 nm, the mean depolarization ratio and also the Lidar Ratio (about 70 sr) for all sites over-flown by the CALIOP sensor onboard the CALIPSO satellite.

In another case study during the dry winter season of 2008, fire plumes attributed to sugar cane fires were frequently observed by IPMet's radars in the absence of rain echoes and documented in terms of radar reflectivity, time and location [12]. On several occasions, IPEN's Elastic Backscatter Lidar in São Paulo observed layers of aerosols of varying strength and heights above the city. The most significant days were selected for calculating

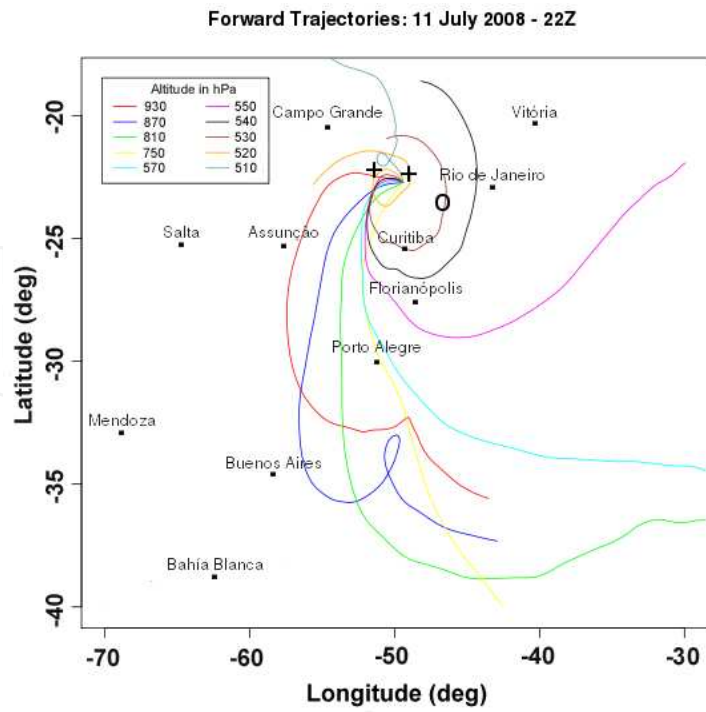


(a)

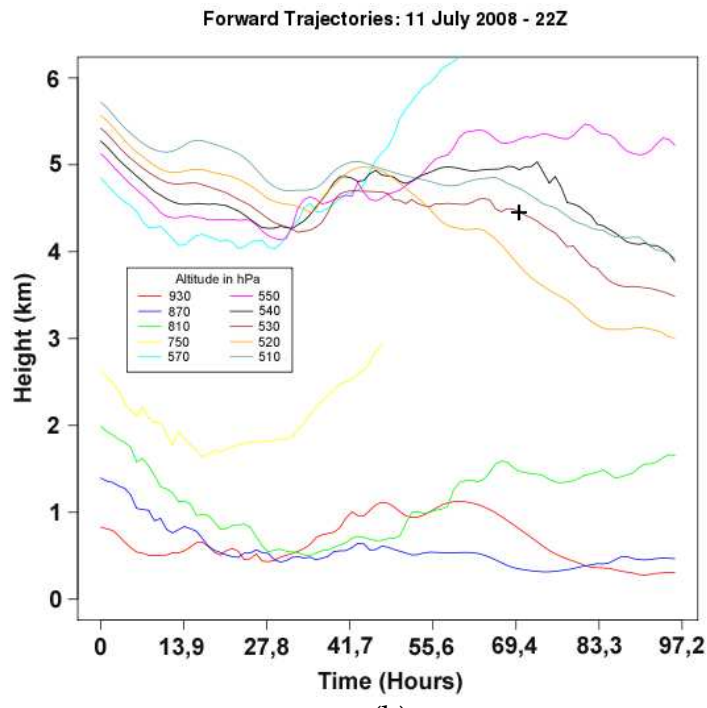


(b)

**Figure 13.** (a) shows the 355 nm Lidar Ratio profile on 10 January 2008 at 00:25 UT (21:25 LT). (b) shows the water vapour mixing ratio extracted on the same day from the 408 nm channel (00:25 UT) and from a radiosonde ascent (00:00 UT).



(a)



(b)

**Figure 14.** Forward trajectories initiated at different heights where a large fire was observed by IPMet’s radars on 11 July 2008, 22:00 UT (19:00 LT). **(a)** The + indicates the position of the PPR and BRU radars; o indicates the position of the lidar in São Paulo (IPEN). **(b)** Forward trajectories plotted against height and time. The + indicates the position of IPEN, marking height and time of arrival matching exactly with the lidar observation (Figure 15).

backward, as well as forward trajectories, deploying the Flextra 3.3 Trajectory Model [81], which was initiated with ECMWF historical data with a  $0,25^\circ \times 0,25^\circ$  grid spacing [12]. The results showed an excellent match between the radar-detected sources of the plumes and lidar observations in São Paulo. Figure 14 presents a typical case study, when emissions from biomass fires were identified by the radars on 11 July 2008 in the central parts of the State, and were subsequently monitored by IPEN's lidar over Metropolitan São Paulo on 14 July 2008, deploying forward and backward trajectories. The forward trajectories, initiated at different heights ranging from 930 hPa (close to ground level) up to 450 hPa (ca 6,7 km amsl) at 30 hPa intervals (only the most significant 10 heights are shown in Figure 14), indicated a transport duration of approximately 70 hours under the prevailing meteorological conditions (Figure 14b). The arrival of the plume over the RMSP on 14 July 2008, as observed by the lidar at IPEN, is shown in Figure 15.

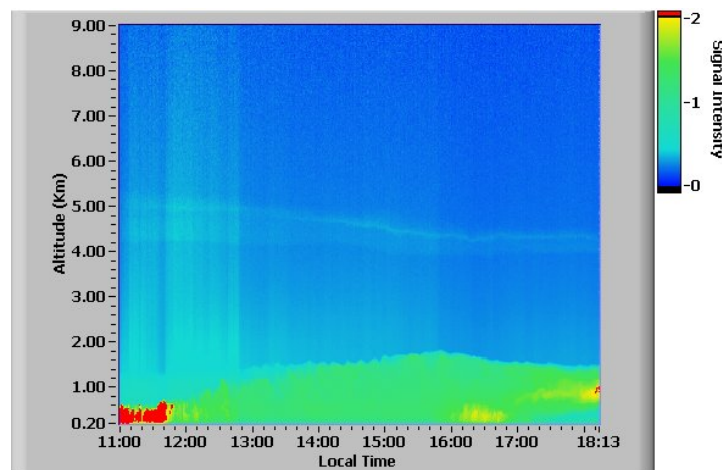
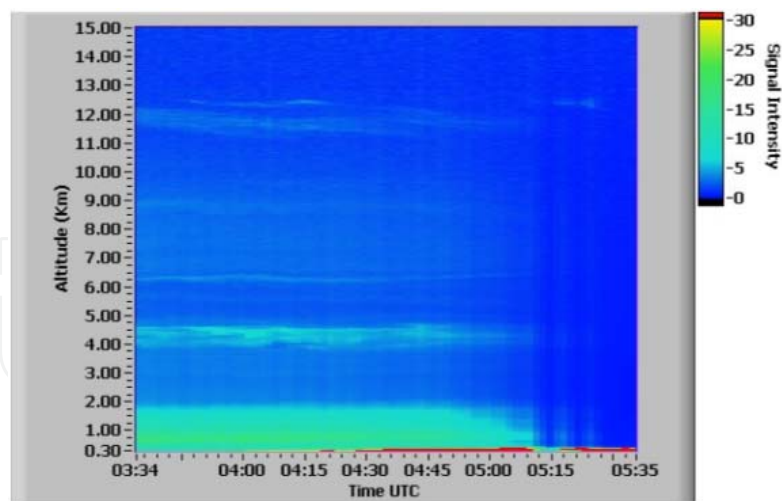


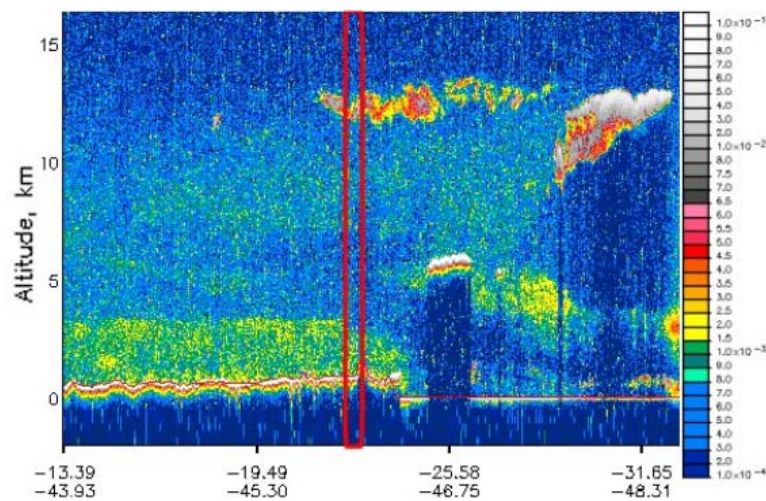
**Figure 15.** Lidar observations at IPEN in São Paulo, showing the range-corrected signal in arbitrary units, on 14 July 2008 between 11:00 and 18:13 LT. The plume identified in Figure 14 can be seen between 4-5 km AGL.

The MSP-Lidar system in São Paulo has also been contributing to CALIPSO satellite validation procedures [75, 82]. During 2007, correlative measurements were carried out with special attention to the dry season (May-October), when most of the days have poor dispersion conditions and long distance transport is more frequent. From a total of 28 days of measurements, on only 10 days were no clouds present below 4 km. Figure 16a presents a typical example, showing the range-corrected signal retrieved by the lidar system at São Paulo on 10 October 2007 between 03:34 and 05:35 UT, which contains the CALIPSO overpass window, beginning at 04:30 UT (Figure 16b). On this day, the closest distance of the satellite ground-track from the lidar site was about 48 km. The presence of aerosol layers above the PBL at 4-5 km, 6 km and 9 km is noticeable. The same features are also observed in the CALIOP 532 nm Total Attenuated Backscattering plot, as shown in Figure 16b. Both systems detected a cirrus structure between 12 and 13 km AGL, but the strong cirrus cloud signal observed in the CALIOP "plot-curtain" is much weaker in the lidar image. The red box in Figure 16b represents the CALIPSO ground-track region over Metropolitan São Paulo with coordinates of  $-22,5625^\circ$  latitude and  $-46,0247^\circ$  longitude at about 04:35 UT.





(a)



(b)

**Figure 16.** (a) Range-corrected lidar signal (plot-curtain) measured by the MSP-Lidar on 10 October 2007, 03:34 - 05:35 UT. (b) Total Attenuated Backscattering signal measured by the CALIOP at 532 nm during the period 04:30 - 04:41 UT on the same day, when it was closest to the MSP-Lidar site (red box).

Figure 17 compares the attenuated backscatter coefficient profile retrieved by CALIOP on board the CALIPSO satellite and the corrected one obtained from the ground-based MSP-Lidar system in São Paulo. The satellite profile has a 5 km horizontal resolution. The attenuated backscatter profile from the MSP-Lidar site was derived under cloud-free conditions from the range-corrected and background noise-subtracted lidar return signal. Both profiles are in good agreement, presenting similar layer patterns in the profiles observed at 5-6 km and about 7 km AGL. Since it can be assumed with reasonable confidence that, at higher altitudes, the horizontal atmospheric structure is more homogeneous, the good agreement between the two systems demonstrates the possibility that they were probing the same air masses for this specific measurement. At lower altitudes, observation of some differences between the two profiles is more likely due to local effects. In this case, the localized effects are more pronounced, and the fact that the systems are not covering the exact same region becomes evident.

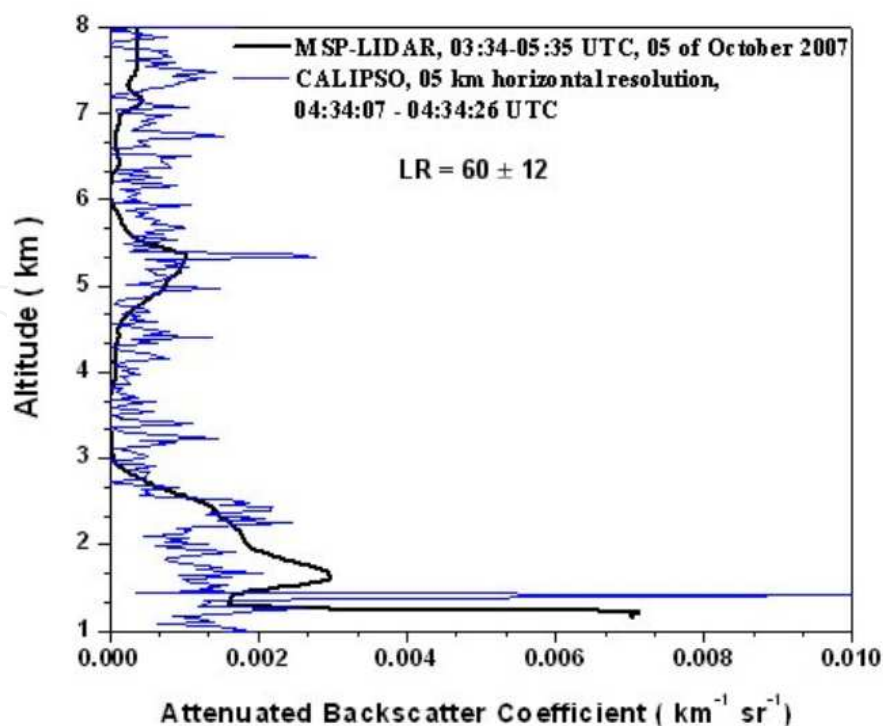


**Figure 17.** Total Attenuated Backscatter Coefficient profiles at 532 nm for the horizontal coverage of CALIPSO level 1 data compared to the Attenuated Backscatter Coefficient retrieved by the ground-based MSP-Lidar system in Metropolitan São Paulo on 10 October 2007.

## 5.2. Mobile Raman lidar

The mobile bi-axial Raman lidar system uses a commercial pulsed Nd:YAG laser, operating at a wavelength of 532 nm in the elastic channel and 607 nm in the Nitrogen Raman channel, with a pulse energy of 130 mJ at 20 Hz PRF. The pulse width is 25 ns, yielding a spatial resolution of 7,5 m. A detailed description of the system is found in [83]. The system allows the determination of the optical properties of the atmosphere, including aerosol backscatter and extinction coefficients, as well as an indication of the type of aerosol present, based on the Lidar Ratio. This lidar has so far been deployed during specific campaigns at three different sites within the central region of São Paulo State, *viz.*, Rio Claro [84], Bauru and Ourinhos [85-87], as well as in Cubatão, an industrial hub at the coast, near Santos [88], as shown in Figure 6.

A one-month pilot study was undertaken during August 2010 in Ourinhos (Figure 6), which is situated in one of the State's major sugar cane producing regions, where biomass burning is a regular occurrence. The objective was to characterize the effects of these emissions on the atmosphere, considering the local circulation and the consequences for the region [85]. In the absence of rain, the plumes were tracked by IPMet's two S-band Doppler radars within their quantitative ranges of 240 km (BRU = Bauru, PPR = Presidente Prudente; Figure 6), using the TITAN (*Thunderstorm Identification, Tracking, Analysis, and Nowcasting*) Radar Software [89]. A large range of meteorological, physical and chemical instrumentation, including the mobile Raman lidar, was used to observe elevated layers and the type of aerosols. A medium-sized

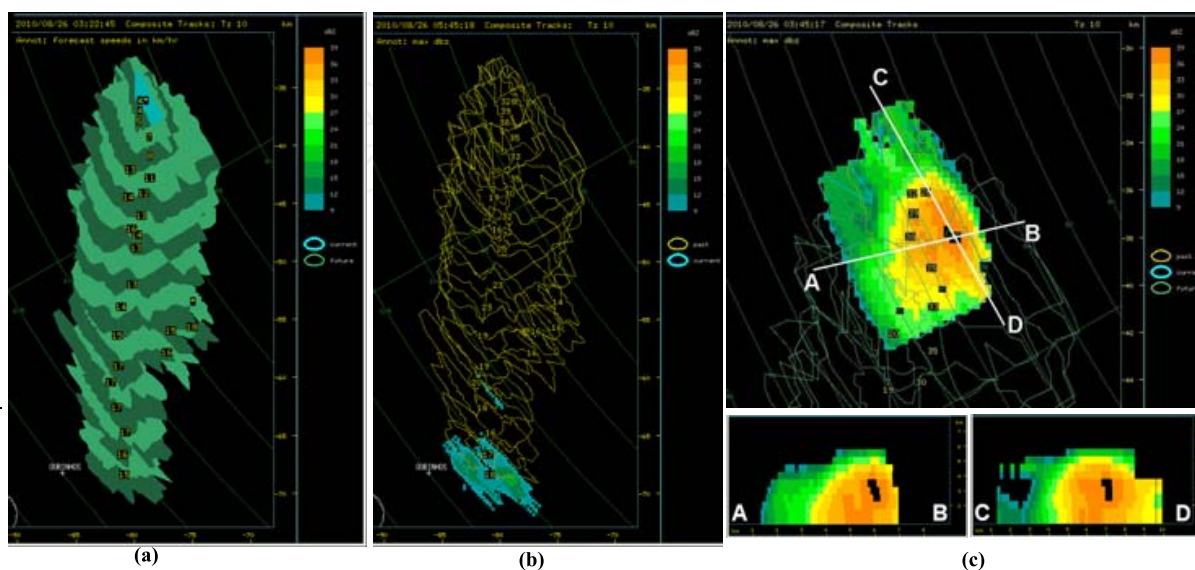
sodar, as well as 6 automatic weather stations, were also deployed in the region. Various gases and aerosol size fractions were sampled, providing an atmospheric chemistry database and thus documenting the impact of the harvesting practice on the region. The aerosol load of the atmosphere was quantified by hourly mean AOD values and hourly mean backscatter profiles. Several case studies have already been analyzed, but the one of 25-26 August 2010 will be shown in this Chapter to illustrate how the various remote sensing instruments are being deployed to generate a complete picture of events.

During the second half of August 2010, the weather was dominated by a high pressure system, resulting in a rise in temperatures, with low humidity favoring the accumulation of pollutants in the atmosphere of the region [25]. IPMet's radars have a 2° beam width and a quantitative range of 240 km, generating a volume-scan every 7,5 minutes, with a resolution of 250 m radially and 1° in azimuth. Reflectivities and radial velocities are recorded at 16 elevations. However, in order to detect and track the biomass burning plumes, a special scanning cycle was configured to provide a better vertical resolution up to the anticipated detectable top of the plumes: 10,0°, 8,0°, 6,5°, 5,0°, 4,0°, 3,2°, 2,4°, 1,6°, 0,8° and 0,3°, with each "sweep" (Plan Position Indicator - PPI) having 360 rays with 957 range bins each. Two different software systems were deployed, *viz.*, IRIS (*Interactive Radar Information System*) Analysis was used first to generate CAPPis (Constant Altitude PPIs) at 1,5 and 2,0 km amsl, in order to identify all smoke plumes within the 240 km range of the radars. Once a plume was identified as likely to pass over the monitoring site, it was tracked using TITAN Software to determine its intensity (based on radar reflectivity in dBZ), horizontal and vertical dimensions, and the velocity of approach. The thresholds used for tracking were 10 dBZ with a minimum volume of 2 km<sup>3</sup>. It should be noted that TITAN uses Universal Time (Local Time LT = UT-3h).

A typical case study of a sugar cane fire in the Ourinhos region is now presented, demonstrating the integration of all types of data into one coherent event. The first echo of a smoke plume was detected by the Bauru radar on 26 August 2010 at 00:08 LT, about 35 km north-northeast of Ourinhos and about 85 km southwest of the radar (Figure 18), rapidly gaining in area and intensity ( $\leq 40$  dBZ near its origin). By 00:22 LT, the TITAN Software could already identify its centroid of  $\geq 10$  dBZ reflectivity and tracked it until 02:45 LT, when the plume had already spread over Ourinhos, where the Raman lidar and sodar were located. As the plume moved southwards with the northerly winds, the aerosols spread out (dispersed) and the reflectivity dropped gradually, but it could still be detected by the radar until 03:46 LT,  $>20$  km south of Ourinhos, using a reflectivity threshold of  $-6$  dBZ [85].

Furthermore, it can be deduced from Figure 18a that while the plume was at a low height during the initial phase of transport, it moved very slowly ( $3-4$  km.h<sup>-1</sup>), since the wind speed in the first few hundred meters was very low ( $\leq 5$  m.s<sup>-1</sup>), as observed by the sodar. There was also a shift of the wind direction from easterly to northerly winds above 300 m AGL. These northerly winds were above the nighttime surface inversion, confirmed by the "Skew T x Log P" profiles of the Meso-Eta model in the 900-800 hPa layer (650–1650 m AGL) as shown in [85]. The vertical velocity ( $w$ ), measured by the sodar, indicated that downward mixing of

the pollutants (aerosols), trapped above the inversion, only commenced at around 09:00-09:30 LT, since from 00:00-09:00 LT the atmosphere was extremely stable below 300 m AGL ( $w = \pm 0 \text{ m.s}^{-1}$ ).



(a) First TITAN centroid of the *queimada* (actual fire, blue) at 03:22 UT (00:22 LT; annotation: propagation velocity in  $\text{km.h}^{-1}$ );

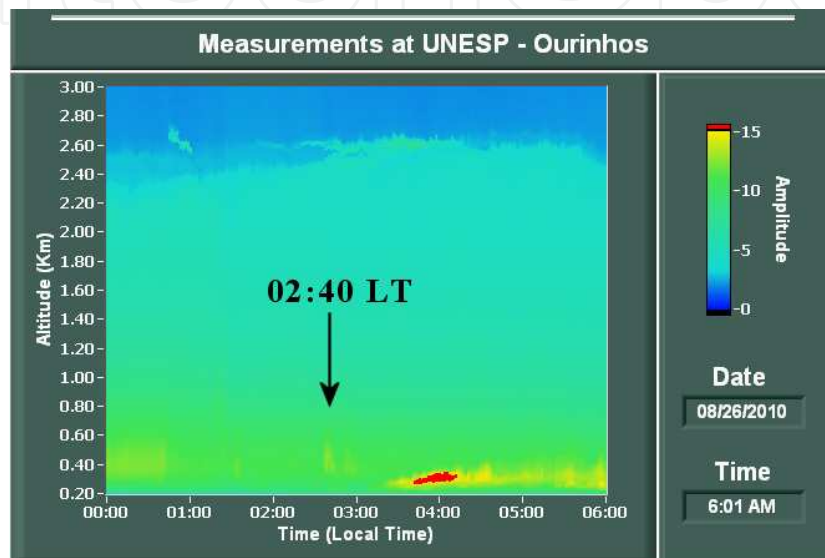
(b) The *queimada* reached the Ourinhos region at 05:45 UT (02:45 LT, blue; annotation: maximum reflectivity in dBZ).

(c) Vertical cross-sections at 03:45 UT (00:45 LT), showing the horizontal and vertical extent along the base lines A-B and C-D.

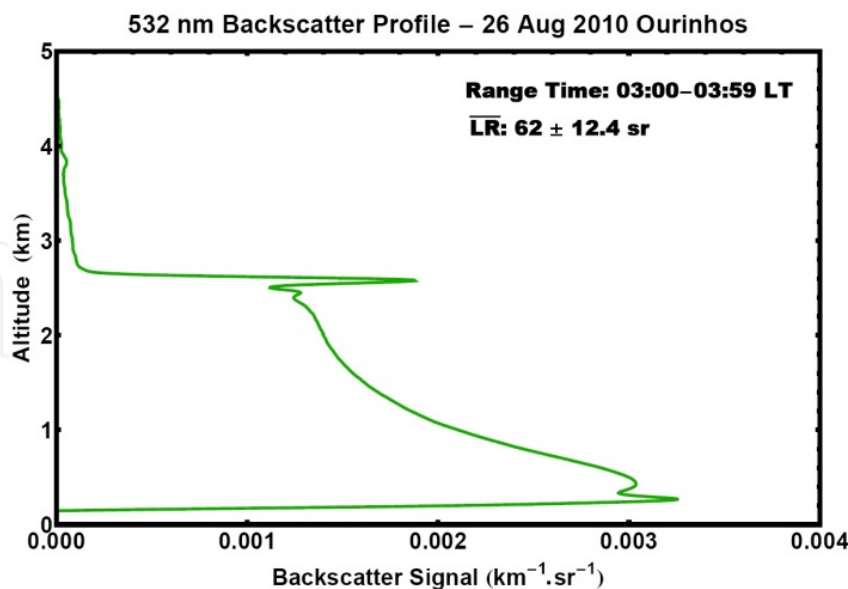
**Figure 18.** Examples of the tracks generated by TITAN on 26 August 2010. The envelopes (10 dBZ reflectivity) show the position of the *queimada* (smoke plume) in intervals of 7,5 min (blue = actual time; green = future; yellow = past).

The lidar observed the arrival of the plume at 02:40 LT between 350 and 600 m AGL (Figure 19a). The top of the PBL extended to about 2,6 km AGL, above which a very dry and relatively warm and clean air mass was advected from the west, creating an elevated inversion which blocked further upward mixing. The lowest layer  $\leq 250$  m AGL appeared clean, being trapped within the surface inversion, inhibiting downward mixing, also confirmed by the sodar measurements, indicating a very stable layer. Lidar data from the Raman Channel (non-elastic signal at 607 nm) were integrated into hourly means until 09:00 LT to obtain the AOD. The results confirmed a high aerosol load of the atmosphere, with hourly mean values of AOD varying between 0,265 and 0,288 until 07:00 LT, after which they increased to 0,433 by 09:00 LT. Hourly means of the Lidar Ratio confirmed the arrival of the plume between 02:00 and 03:00 LT (example shown in Figure 19b), while an almost 20% increase of LR to 72 sr after 07:00 LT was probably due to downward mixing of the aerosols accumulated above the inversion, also confirmed by an increase of AOD values from the Raman signal [85]. LR values of around 70 sr suggest aerosols originating from biomass burning [90, 91].

Visual images from overpasses of the MODIS-AQUA satellite on 25 and 26 August 2010 (at 17:35 and 16:40 UT, respectively; 14:35 and 13:40 LT) showed intense smoke plumes to the west and south of the Ourinhos region, with AOD values of up to about 1,0. In the Ourinhos region, the AOD increased during the period 25-26 August, from about 0,2 to about 0,6 (Figure 20a), which is in agreement with the early afternoon lidar measurements (Figure 20b), which provided an AOD value of 0,380 during the period from 13:00 to 14:00 LT.

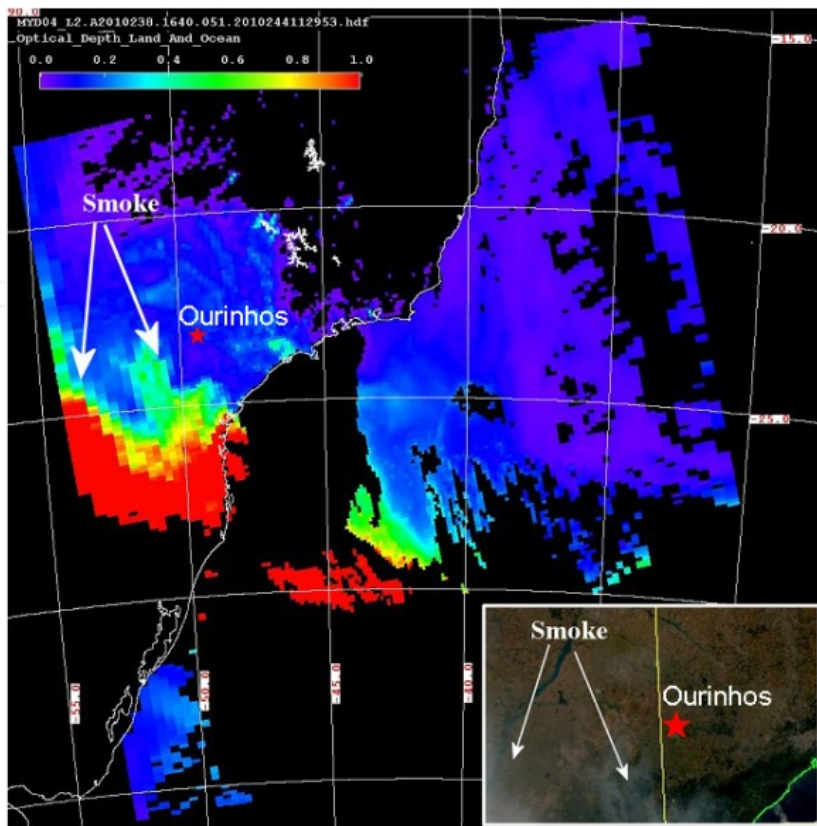


(a)

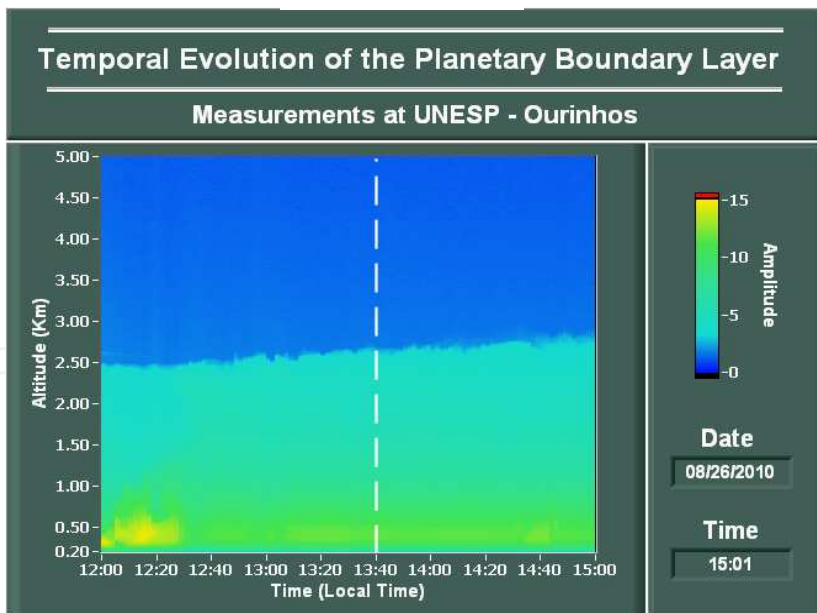


(a)

**Figure 19.** (a) Lidar signal (arbitrary units) visualized for 00:00-06:00 LT, up to 3 km AGL. (b) Backscatter Profile at 532 nm for the hourly mean period 03:00-03:59 LT on 26 August 2010.



(a)



(b)

**Figure 20.** (a) AOD image from MODIS-AQUA on 26 August 2010, 16:40-16:45 UT (13:40-13:45 LT). The inset shows a simultaneous visual image of the Ourinhos region.

(b) Lidar measurements on 26 August 2010, 12:01-15:01 LT. The time of the MODIS-AQUA overpass is indicated by the dashed white line.

Aerosols collected during daytime and nighttime periods at the lidar site [85-87, 92], using low-volume filter samplers, were chemically characterized by means of ion chromatography. A higher concentration of  $K^+$  during the period from 22:00 on 25 August to 16:00 on 26 August 2010 indicated the presence of biomass-burning material (Figure 21), since  $K^+$  is a plant macronutrient released during the combustion process. Levoglucosan, a very specific chemical marker of biomass combustion, was well above average concentration during day sampling on 26 August and even higher during the following night, indicating a strong presence of biomass smoke on both days.

In the study region, ions such as magnesium ( $Mg^{2+}$ ) and calcium ( $Ca^{2+}$ ) are associated with the re-suspension of soil dust, which often accompanies biomass fires due to the intense updrafts created. On 26 August, concentrations of these species were higher during the daytime, due to the increased emissions from barren fields and unsealed roads associated with higher wind speeds (Figure 21).

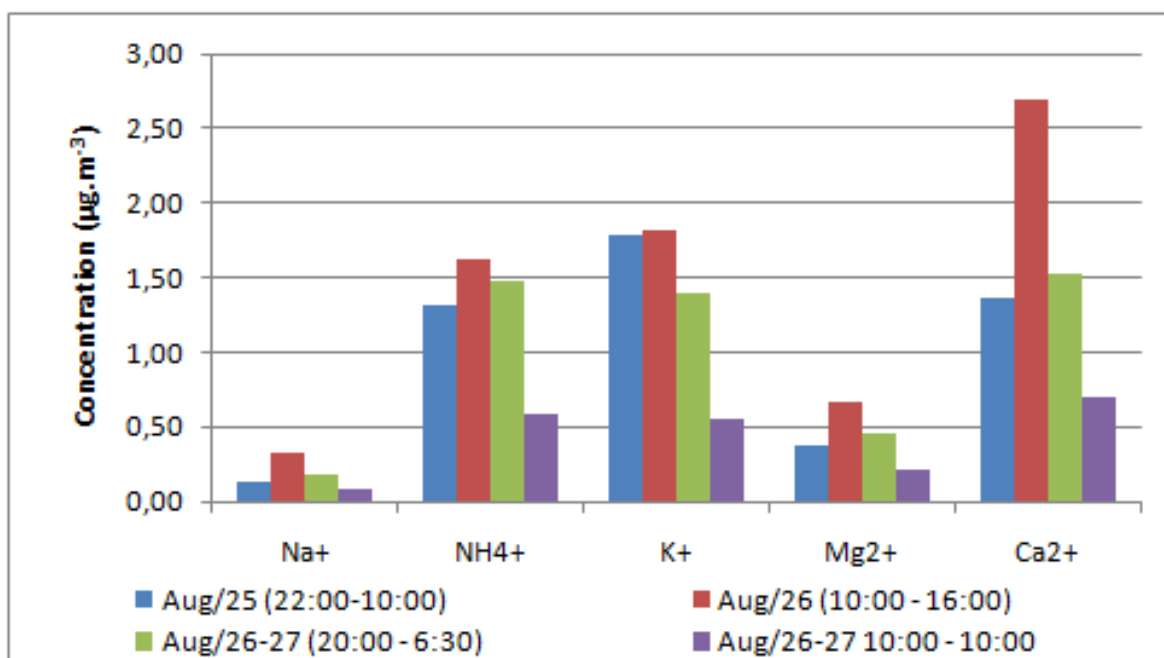


**Figure 21.** Soluble major cation concentrations for the period 25-27 August 2010 (sampling periods are indicated in local time; after [85]).

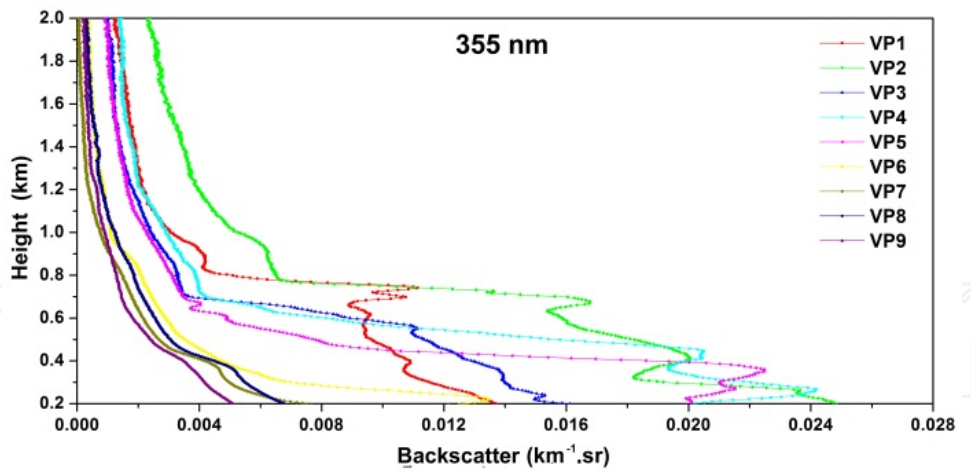
Further evidence of the impact on the Ourinhos region of emissions from sugar cane fires was obtained by comparing the concentrations of organic compounds in aerosol particles collected on 26 August with those collected one day earlier. Ambient levels of polycyclic aromatic hydrocarbons (PAH), as well as PAH derivatives, such as oxy-PAH, were significantly higher on 26 August 2010 than on the previous day, confirming that emissions from sugar cane fires affected the urban atmosphere of Ourinhos.

### 5.3. Scanning lidar in Cubatão

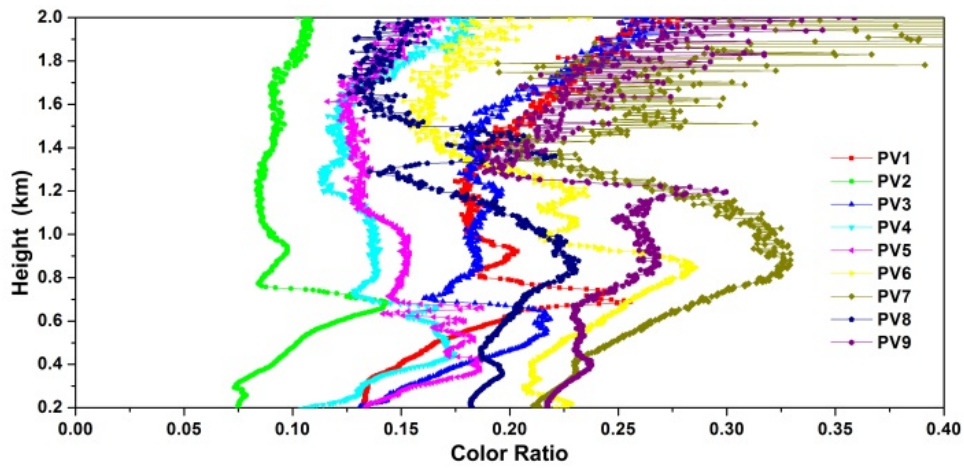
An elastic backscatter lidar system, with similar characteristics to the mobile lidar, was installed in 2011 at CEPEMA-USP (*Centro de Pesquisas em Meio Ambiente*, a Center for Environmental Research and Training, under the responsibility of the Universidade de São Paulo) in the Cubatão industrial area, with the ultimate goal of remotely monitoring industrial emissions. It also uses a commercial pulsed Nd:YAG laser, operating at three wavelengths (355, 532 and 1064 nm) with pulse energies of 100, 200 and 400 mJ, respectively, at 20 Hz PRF. A detailed description of the system and its location is found in [33]. The system allows the determination of the optical properties of the atmosphere, including aerosol backscatter and extinction coefficients, as well as an indication of the type of aerosol present, based on the Lidar Ratio. The lidar is co-located with a sodar / RASS system and an air quality monitoring station.

During May 2011, the system was deployed in a vertical pointing mode during an intensive field campaign. A 24-hour period was selected that demonstrated the complexity of the local situation, which is dominated by topographical effects and prevailing meteorological conditions [33]. Vertical profiles of the Backscatter Coefficient (BSC) and the Colour Ratio were calculated for 30-minute periods from 17:30 – 19:59 and 21:42 – 23:36 LT. The BSC was highest for all frequencies between 19:30 and 19:59 LT (Figure 22a), indicating a strong inflow of aerosols, while after 21:42 LT the BSC showed much lower values (Figure 22b), representing a relatively clean air mass. At the same time, the Colour Ratio between all frequencies increased significantly, indicating the presence of small particles, especially between 0,8 and 1,3 km AGL [33]. Ground-level observations of PM<sub>10</sub> and PM<sub>2.5</sub> for the 24-hour period indicate that PM<sub>10</sub> concentrations were almost twice as high as those of PM<sub>2.5</sub> until about 18:00 LT (Figure 23). During the same period, the sodar observed extremely low wind speeds from varying directions. However, this resulted in very stable PBL conditions, and a temperature inversion began to develop from 18:30 onwards, reaching its greatest depth and intensity at 21:30. Thereafter, it gradually dropped in height and began to erode, as the air flow from the interior intensified, until it totally dissipated by 01:00 LT [33], due to the katabatic warming of the descending northerly airflow, which then also reduced the aerosol concentrations at ground level (Figure 23). Figure 24a shows the development of the surface inversion at 20:00 LT, overlaid by warm air flowing from the interior, with simultaneous downward motion below 240 m AGL (Figure 24b), highlighting the complex interaction of meteorology and topography in this region. This situation clearly demonstrates the need for solid environmental impact studies *before* locating industrial developments, in order to avoid any negative health impacts in the local population due to the accumulation of pollutants.





(a)



(b)

**Figure 22.** (a) Vertical profile of Backscatter Coefficient (BSC) at 355 nm; (b) Colour Ratio 532/355 nm. (After [33]).

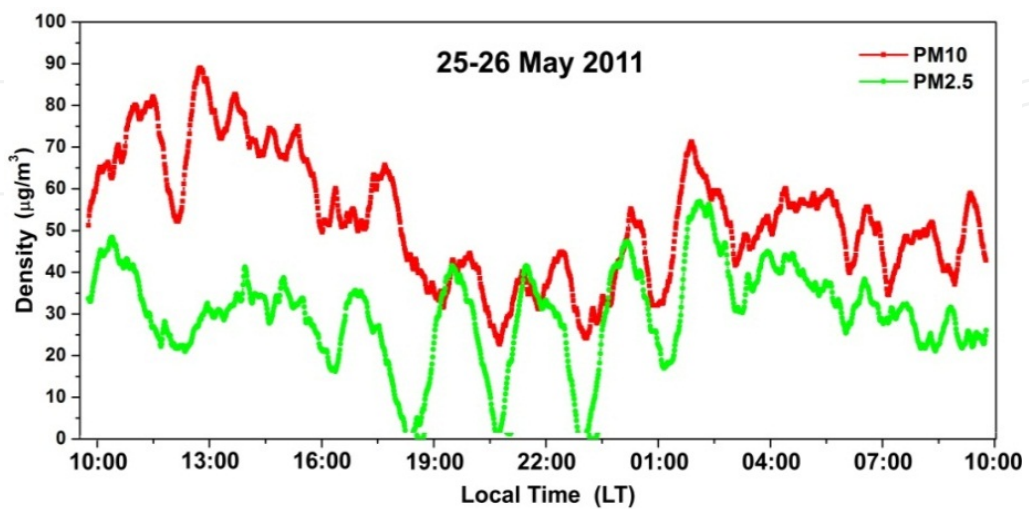
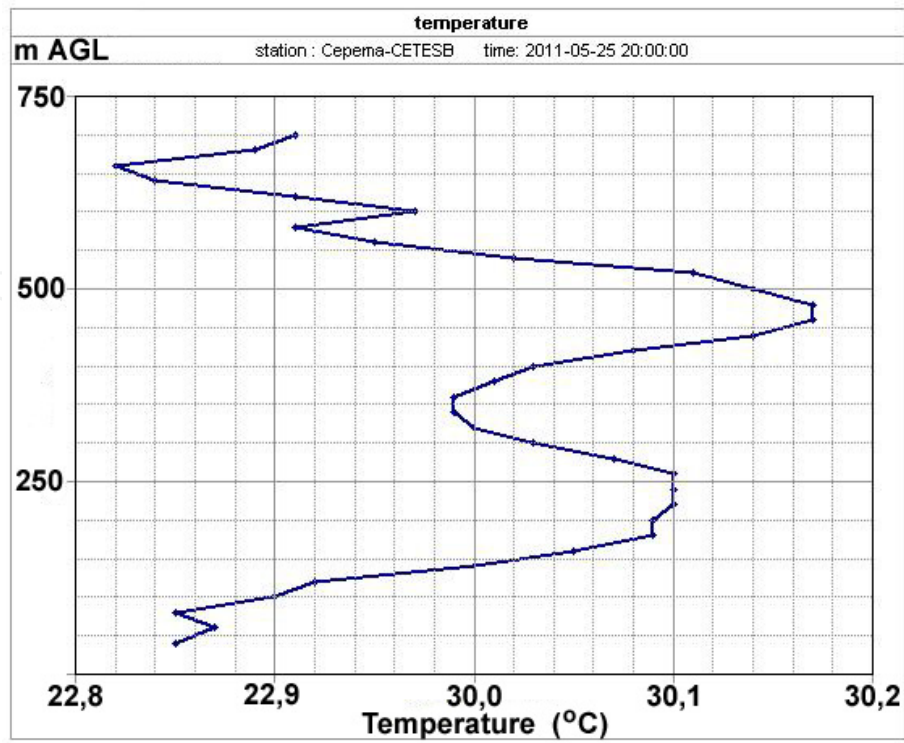
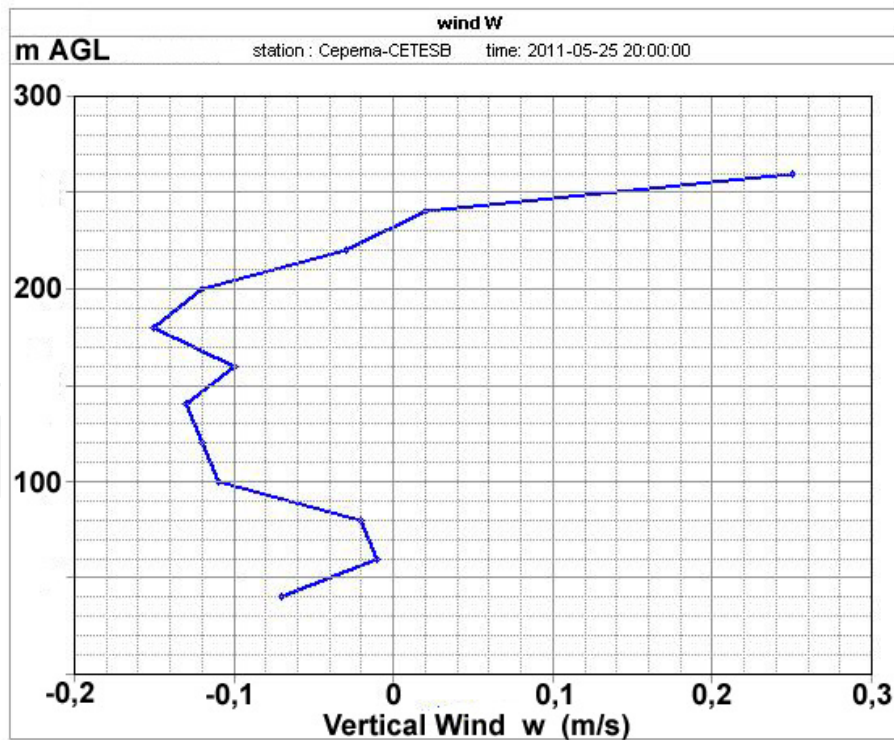


**Figure 23.** Concentrations of  $\text{PM}_{10}$  and  $\text{PM}_{2.5}$  from 10:00 LT on 25 May to 10:00 LT on 26 May 2011. (After [33]).



(a)



(b)

**Figure 24.** Sodar/RASS measurements on 25 May 2011, mean profiles for 19:30-20:00 LT. **(a)** Vertical profile of temperature; **(b)** Vertical profile of vertical wind velocity.

## 6. Impacts of aerosols

### 6.1. Impact of aerosols on human health

The impact of anthropogenic aerosols on human health has been acknowledged in both metropolitan and rural regions [93, and references therein]. In general terms, as pointed out in [93], in recent years the population of São Paulo State has suffered from either acute (short-term, high concentration) or chronic (long-term, lower concentration) exposure to particulate air pollutants, depending on location. In rural regions, there is acute exposure to high concentrations of biomass burning particulates present in plumes, as well as chronic exposure to these aerosols on a regional basis throughout the dry season. In metropolitan São Paulo, there is chronic exposure to particulates derived from road transport and industrial emissions, together with periodic acute exposure to extremely high levels of pollutants under conditions of thermal inversions and stationary air masses [94-96].

There have been many studies of the correlation between aerosol concentrations and human health impacts in the metropolitan regions, especially in São Paulo city [97-102]. Typical effects include asthma and pneumonia, as well as other cardiovascular and respiratory symptoms. Increased levels of PM<sub>10</sub> were associated with increases of 6,7% and 2,2% in hospital admissions of children due to respiratory illness [96, 103]. Increments of 10 µg.m<sup>-3</sup> in PM<sub>10</sub> concentrations resulted in increases in hospital admissions of between 0,9% and 6,7% in Sao Paulo [97, 103-105]. In the elderly, a 5,4% increase in the number of deaths was linked to a 10 µg.m<sup>-3</sup> increase in PM<sub>10</sub> [105]. Industrial emissions in Cubatão have been found to seriously affect the lung function of children, with respiratory airflow rates correlated with PM<sub>10</sub> concentrations obtained for the preceding month [106].

Bourotte *et al.* [56] investigated the relationships between peak expiratory flow (PEF) measurements and soluble ions in fine and coarse aerosols, and found a negative correlation between PEF and the coarse fraction ions Cl<sup>-</sup>, Na<sup>+</sup>, Mg<sup>2+</sup> and NH<sub>4</sub><sup>+</sup>, as well as between PEF and fine fraction Mg<sup>2+</sup>. The findings suggested that increased levels of coarse particles could be of especial concern for asthmatic individuals.

In these heavily polluted regions, atmospheric particles contain components known to be carcinogenic and mutagenic, including ketones, aldehydes, quinolines, carboxylic acids, polycyclic aromatic compounds (PAHs), and nitro-PAHs. These substances have been associated with exhaust emissions from road vehicles in southeast Brazil [69, 107-109]. Benzo[a]pyrene equivalent values suggest that the cancer risk is greater for the São Paulo city aerosol than elsewhere in the State, although concentrations may not exceed World Health Organization guidelines [65].

Biomass burning emissions in rural regions also have a recognized influence on human health, as well as environmental impacts including modification of nutrient cycling [10, 11, 47], and effects on climate including alterations of the radiative properties of the lower atmosphere, cloud formation and precipitation [110, 111]. For these reasons, as well as due to the need to meet certification requirements of importing countries, there has been

increased pressure for mechanization of harvesting, since the mechanized process does not necessarily require prior burning of the crop. Nonetheless, until recently burning has continued to be employed in mechanized areas (using simpler machinery) because it can improve economic efficiency by around 30-40% [50, 112].

A clear relationship between particulate air pollution and the occurrence of respiratory illness in sugar cane burning regions of the State has been reported [45, 113-116]. Particulate material from sugar cane burning was demonstrated to have the greatest detrimental effect on the respiratory systems of the most sensitive population groups. Cançado *et al.* [45] measured black carbon and trace elements in fine and coarse aerosol fractions, and related the concentrations to daily records of hospital admissions for respiratory illness of children (<13 years old) and the elderly (>64 years), in the town of Piracicaba. Increases of  $10,2 \mu\text{g}\cdot\text{m}^{-3}$  ( $\text{PM}_{2.5}$ ) and  $42,9 \mu\text{g}\cdot\text{m}^{-3}$  ( $\text{PM}_{10}$ ) were associated with increases in hospital admissions of 21,4% (children) and 31,03% (elderly people).

Carcinogenic and mutagenic compounds are emitted during biomass burning [109]. Concentrations of PAHs in a rural sugar cane burning region during the harvest period were in the range  $0,5\text{-}8,6 \text{ ng}\cdot\text{m}^{-3}$  [38]. The mutagenic activity of  $\text{PM}_{10}$  was much higher during the harvest season, when the  $\text{PM}_{10}$  concentration was  $67 \mu\text{g}\cdot\text{m}^{-3}$ , and the mutagenic potency was  $13,45 \text{ revertants m}^{-3}$ . During the summer (non-burning period), the  $\text{PM}_{10}$  concentration was  $20,9 \mu\text{g}\cdot\text{m}^{-3}$ , and the mutagenic potency was  $1,30 \text{ revertants m}^{-3}$  [117].

## 6.2. Impact of aerosols on rainfall

Aerosols derived from all of the sources described above are able to alter the radiative properties of the troposphere, and can modify the processes that lead to the development of cloud condensation nuclei, cloud droplets, and ultimately precipitation [118-120]. The magnitudes of these effects depend on the size distribution, number concentration and chemical composition of the particles, and can therefore vary widely within the same region.

Dufek and Ambrizzi [121] used daily precipitation data collected at 59 locations in São Paulo State to investigate rainfall trends for the period 1950-1999. Although some of the findings were contradictory, an overall trend towards a wetter climate was identified, with rainfall concentrated into a smaller number of more intense events. It was suggested that these changes could be related to the presence of biomass burning aerosols, as well as changes in land use. Evidence that the aerosols probably act as cloud condensation nuclei was provided in [122], where a relationship was identified between water-soluble organic carbon (WSOC) in the particles and dissolved organic carbon (DOC) in rainwater.

An important point is that sugar cane production in São Paulo State has increased over this period. Between the 1990/91 and 2000/01 seasons, the harvest increased from 132 Mt to 194 Mt [123]. It can therefore be supposed that there was also a large increase in emissions of aerosols from the burning of the crop, since manual harvesting of the cane (which requires

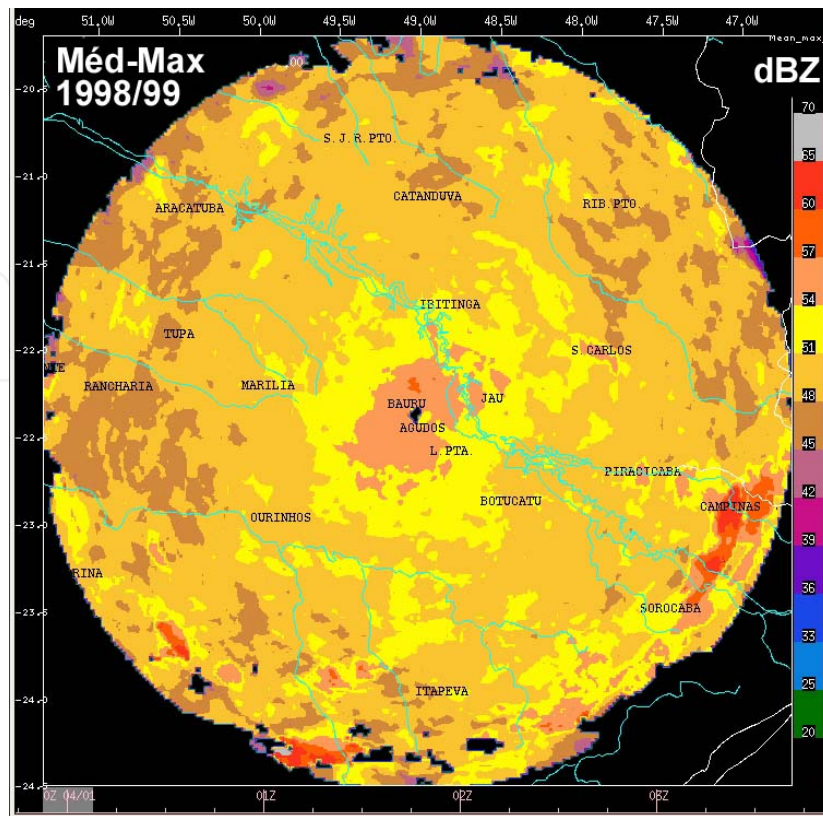
prior burning) was the norm over the period. Mechanization of the crop (which does not involve burning) has only been introduced recently (from around 2005). The main conclusion to be drawn from this is that the trend towards a smaller number of more intense precipitation events, as reported in [121], could now be reversed in the interior of São Paulo State, as sugar cane burning is progressively phased out.

The climatological characterization of storm properties, such as area, volume, maximum echo top and reflectivity during two summer seasons, *viz.*, 1998-1999 and 1999-2000, based on observations from the Bauru S-band Doppler radar, has for the first time shown the spatial distribution of these parameters in central São Paulo State. Gomes and Escobedo [124] showed that some preferential areas of precipitation, taking into account a precipitation envelope area defined by the 25 dBZ threshold, were located along the Tietê River valley. The mean maximum reflectivity field (>40 dBZ), representing the cores of convective precipitation systems, has highlighted some preferential regions for convection to develop over urban and industrialized areas, such as metropolitan Campinas (Figure 25a). A climatology of flash density (Figure 25b; [21]) also identified Campinas as one of three regions with a higher concentration of lightning discharges, attributed to the occurrence of heat islands due to anthropogenic activities. Thus, the spatial distribution of the reflectivity field exceeding 40 dBZ in the Campinas region reinforces results showing a strong correlation between the frequency of cloud-to-ground lightning strokes and precipitation intensity.

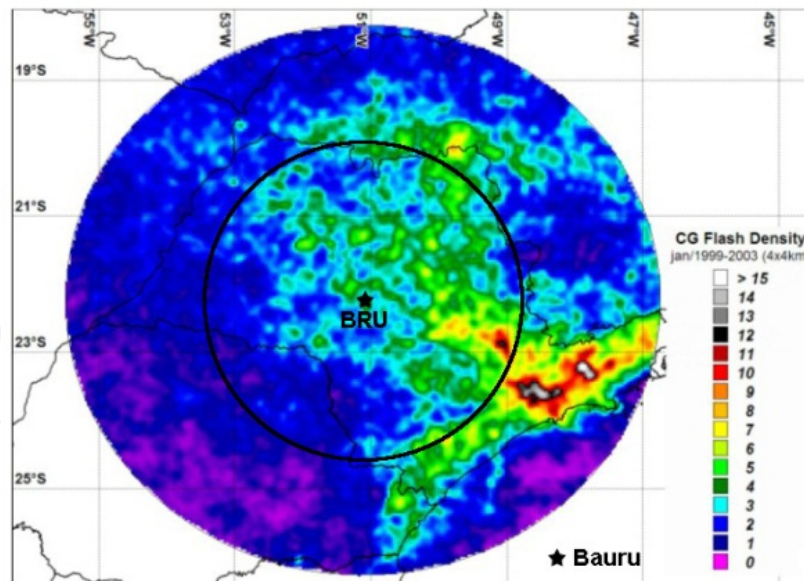
The influence of anthropogenic aerosols on precipitation patterns in the region is the subject of research currently in progress as part of a thematic climate change research programme sponsored by FAPESP (the São Paulo State Research Foundation). The quantitative evaluation of changes in the rainfall pattern, such as increases or decreases of area rainfall totals, number and volume of convective cells, duration of rain events, distribution of echo top heights, etc., is in progress for a 10-year period of integrated radar observations (Bauru and Presidente Prudente radars), using the TITAN Software.

### **6.3. Impact of aerosols on the frequency of lightning**

Westcott [125] documented for the first time an impact of large cities on the cloud-to-ground (CG) lightning frequency in the Midwest of the United States. This was followed up by various researchers around the world, including in Brazil [20] and ultimately summarized in [22], using 10 years of observations from the Brazilian Lightning Detection Networks (1999-2008). This research confirmed the impact of anthropogenic activities on lightning, but it also highlighted the complexity of the correlation between urban heat islands, concentrations of PM<sub>10</sub> and SO<sub>2</sub> in terms of weekly cycles and meteorological conditions, such as CAPE (Convective Available Potential Energy) and other microphysical parameters. One of the most important findings was that the CG frequency increases with increasing concentrations of PM<sub>10</sub> up to a certain threshold of PM<sub>10</sub> concentration (saturation), after which it decreases with further increases of PM<sub>10</sub> concentrations. As the CG frequency increases due to urban impacts, the percentage of positive strokes is reduced.



(a)



(b)

**Figure 25.** (a) Spatial distribution of the average maximum reflectivity (dBZ), during the period October 1998 to March 1999. TITAN storm threshold was defined as reflectivity >40 dBZ within the 240 km range of the Bauru Doppler radar (after [124]). (b) Flash density within the 450 km range of the Bauru radar (after [21]). The circle indicates the 240 km quantitative range as in the TITAN image above.

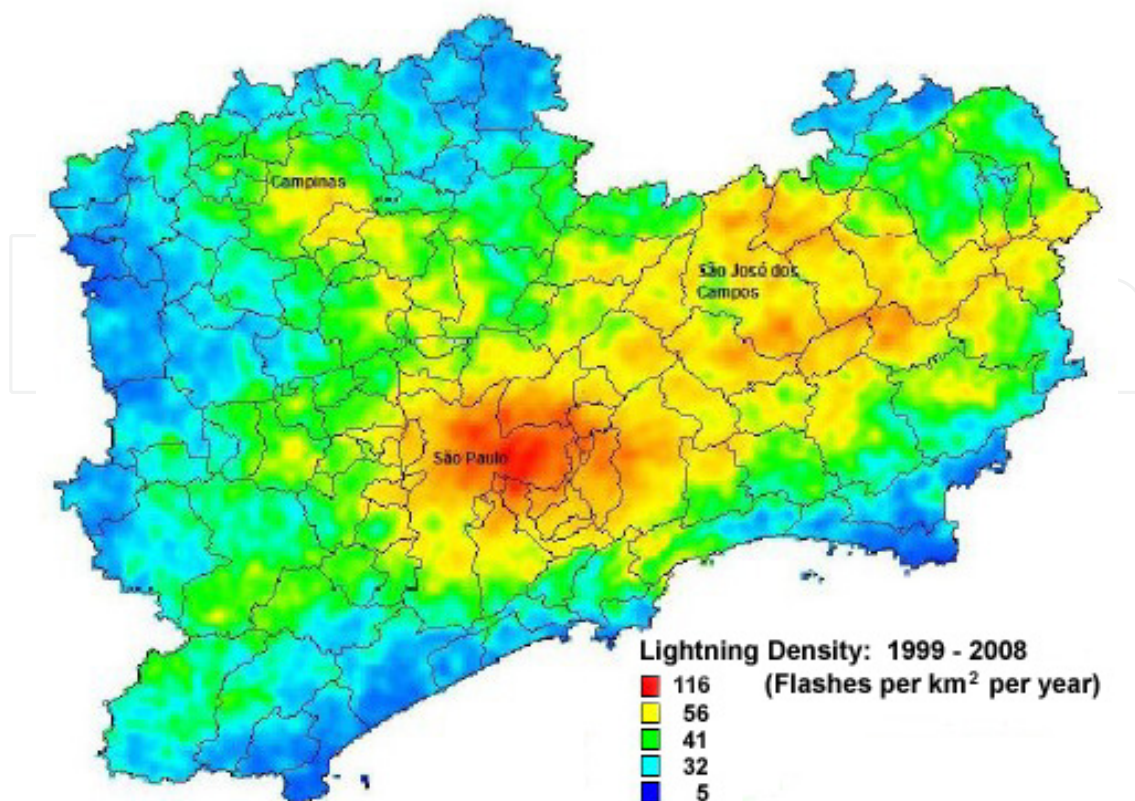


**Figure 26.** Lightning density (flashes per km<sup>2</sup> per year) during the period 1999 - 2008 for the eastern part of the State of São Paulo, which includes the major urban complexes, as well as the highly industrialized Paraíba Valley (after [22]).

## 7. Final considerations

This Chapter provides a review of all relevant historical data concerning the nature, concentrations and impacts of atmospheric aerosols in southeast Brazil. Highlights are the characterization of chemical, physical and optical properties of aerosols, as well as their geographic distribution within the State of São Paulo.

A significant reduction of mean annual PM<sub>10</sub> concentrations could be noticed from 1998 onwards, confirming the success of the implementation of stringent air quality control measures, administered by CETESB. However, within the industrial suburb of Cubatão, confined in a valley, concentrations are still about twice the PQAr. After 2002, the annual mean PM<sub>10</sub> concentrations in the RMSP and the interior of the state show relatively little year to year variation, but remain mostly below the Annual Standard (PQAr = 50 µg.m<sup>-3</sup>).

At present, sugar cane burning, together with the re-suspension of soil dust that is inevitable during the harvesting process, is a major influence on aerosol concentrations, size distribution and dry deposition in rural regions of São Paulo State. However, in this region (and elsewhere in Brazil), the practice of pre-harvest burning is being eliminated. Recent legislation (State Law no. 11.241/02) envisages the complete cessation of the practice in mechanizable areas by 2021 and in non-mechanizable areas by 2031. Furthermore, an

agreement between sugar cane producers and the State government has been reached, which involves elimination of burning in mechanizable areas by 2014, and in non-mechanizable areas by 2017 [9, 126]. This will have major environmental implications, including improvements in air quality and changes in the rates of deposition of nutrient species from the atmosphere to vegetation, soils and freshwater bodies [10]. Nonetheless, at present burning continues in 44% of the area planted with sugar cane [9]. Tsao *et al.* [127] suggest, using a life cycle analysis, that pollutant emissions in sugar cane regions are still increasing, due an expansion of the planted area, and that the burning step still contributes the largest fraction of the total emission.

Improvements in air quality in the metropolitan regions are likely to proceed at a slower pace than in the interior of the State, largely due to the dominant influence of emissions from the road transport sector. Nonetheless, emissions of aerosols and other pollutants are ultimately expected to be attenuated following progressive modernization of the vehicle fleet, and implementation of better controls on emissions from both vehicular and industrial sources.

Examples of case studies presented have demonstrated the capability of weather radars to detect, track and quantify emissions from biomass fires in the absence of rain echoes, deploying a special elevation scanning procedure to generate Volume-Scans every 7,5 min. Furthermore, satellites orbiting with lidar systems on board (e.g., MODIS-AQUA, CALIPSO, CloudSat) also have the capability to detect and quantify optical properties of aerosols.

With the gradual introduction of lidars in Brazil during recent years, it has also become possible to quantify in situ the vertical distribution and optical properties of suspended aerosols. However, in the State of São Paulo there are currently only three lidar systems available, *viz.*, one fixed lidar each in São Paulo city and in Cubatão, supplemented by the mobile lidar for periodic deployment in the interior of the State. Additional fixed lidar installations are therefore suggested for Campinas, Rio Claro, Bauru and São José do Rio Preto (situated in an important sugar cane production region in the north of the State) as a minimum configuration for a network, together with a second mobile system in São José dos Campos to cover the industrial activities in the Paraíba Valley.

## Author details

Gerhard Held and Ana Maria Gomes

*Instituto de Pesquisas Meteorológicas, Universidade Estadual Paulista, Bauru, S.P., Brazil*

Andrew G. Allen and Arnaldo A. Cardoso

*Instituto de Química, Universidade Estadual Paulista, Araraquara, S.P., Brazil*

Fabio J.S. Lopes and Eduardo Landulfo

*Centro de Lasers e Aplicações, Instituto de Pesquisas Energéticas e Nucleares, Universidade de São Paulo, São Paulo, S.P., Brazil*



## 8. References

- [1] TRACE-A (1992). [http://www-gte.larc.nasa.gov/trace/tra\\_hmpg.htm](http://www-gte.larc.nasa.gov/trace/tra_hmpg.htm)
- [2] Lindesay J A, Andreae M O, Goldammer J G, Harris G, Annegarn H J, Garstang M, Scholes R J, van Wilgen B W (1996). International Geosphere-Biosphere Programme/International Global Atmospheric Chemistry SAFARI-92 field experiment: Background and overview, *J. Geophys. Res.*, 101, D19, 23,521-23,530.
- [3] LBA (2012). <http://lba.inpa.gov.br/lba/#>
- [4] Kocinas S, Artaxo P (1992). O monitoramento contínuo de elementos traços em aerossóis atmosféricos da bacia Amazônica. *Proceedings, VII CBMET*, São Paulo, 901-903. <http://www.cbmet.com/cbm-files/19-02759b1503f7d21b92c9a5774714f2ba.pdf>
- [5] Allen A G, Cardoso A A, Da Rocha G O (2004). Influence of sugarcane burning on aerosol soluble ion composition in Southeastern Brazil. *Atmos. Environ.*, 38, 5025-5038.
- [6] Da Rocha G O, Allen A G, Cardoso A A (2005). Influence of agricultural biomass burning on aerosol size distribution and dry deposition. *Environ. Sci. Technol.*, 39, 5293-5301.
- [7] Lara L L, Artaxo P, Martinelli L A, Victoria R L, Ferraz E S B (2005). Characteristics of aerosols from sugar-cane burning emissions in Southeastern Brazil. *Atmos. Environ.*, 39, 4627-4636.
- [8] IBGE (2011). Levantamento Sistemático da Produção Agrícola. Instituto Brasileiro de Geografia e Estatística (IBGE), Rio de Janeiro, December 2011: ISSN 0103-443X.
- [9] CETESB (2012). Relatório 2011: Qualidade do Ar no Estado de São Paulo. CETESB, São Paulo, 124p. <http://www.cetesb.sp.gov.br/ar/qualidade-do-ar/31-publicacoes-e-relatorios>
- [10] Allen A G, Cardoso A A, Wiatr A, Machado C M D, Paterlini W C, Baker J (2010). Influence of intensive agriculture on dry deposition of aerosol nutrients. *J. Braz. Chem. Soc.*, 21, 87-97.
- [11] Allen A G, Machado C M D, Cardoso A A (2011). Measurements and modeling of reactive nitrogen deposition in southeast Brazil. *Environ. Pollut.*, 159, 1190-1197.
- [12] Held G, Landulfo E, Lopes F J S, Arteta J, Marecal V, Bassan J M (2011). Emissions from sugar cane fires in the central & western State of São Paulo and aerosol layers over metropolitan São Paulo observed by IPEN's lidar: Is there a connection? *Opt. Pura Apl.*, 44, 83-91.
- [13] Orsini C M Q, Artaxo P (1983). Algumas características da matéria particulada inalável em Cubatao. In: *Seminário sobre uma Síntese do Conhecimento sobre a Baixada Santista*, CETESB, São Paulo, SP, 1983, 516p.
- [14] Andrade M F, Orsini C, Maenhaut W (1994). Relation between aerosol sources and meteorological parameters for inhalable atmospheric particles in Sao Paulo City, Brazil. *Atmos. Environ.*, 28, 2307-2315.
- [15] Wikipedia (2011). [http://en.wikipedia.org/wiki/Largest\\_cities\\_in\\_the\\_world](http://en.wikipedia.org/wiki/Largest_cities_in_the_world) (Accessed in December 2011).
- [16] IBGE (2010). [http://www.censo2010.ibge.gov.br/resultados\\_do\\_censo2010.php](http://www.censo2010.ibge.gov.br/resultados_do_censo2010.php) (Accessed in December 2011).

- [17] Saldiva P H N, Pope C A, Schwartz J, Dockery D W, Lichtenfels A J, Salge J M, Barone I, Bohm G M (1995). Air pollution and mortality in elderly people: A time-series study in São Paulo, Brazil. *Arch. Environ. Health*, 50, 159–163.
- [18] RINDAT (2012). <http://www.rindat.com.br/>
- [19] ELAT/INPE (2012). <http://www.inpe.br/webelat/homepage/>
- [20] Naccarato K P, Pinto Jr O, Pinto I R C A (2003). Evidence of thermal and aerosol effects in the cloud-to-ground lightning density and polarity over large urban areas in Southeastern Brazil - Overview and Comparison to the Campaign Period. *Geophysical Res. Letters*, 30, 13, 1674-1677, doi: 10.1029/2003GLO17496.
- [21] Naccarato K P, Pinto Jr O, Held G, 2004. Climatology of Lightning in Brazil - Overview and Comparison to the Campaign Period. *Proceedings, HIBISCUS / TroCCiBras / TROCINOX Workshop*, Bauru, SP, 16-19 November 2004, p10. [http://www.ipmet.unesp.br/ipmet\\_html/troccibras/publicacoes.html](http://www.ipmet.unesp.br/ipmet_html/troccibras/publicacoes.html)
- [22] Gomes W R (2010). Estudo das características da atividade dos raios na região metropolitana de São Paulo. PhD thesis, Geofísica Espacial, INPE, São José dos Campos, Brazil, 157p.
- [23] INMET (2012). <http://www.inmet.gov.br/html/clima/mapas/?mapa=prec>
- [24] Kousky V E (1988). Pentad outgoing longwave radiation climatology for the South American sector. *Rev. Bras. Meteor.*, 3, 217-231.
- [25] Held G, Nery J T, Gomes A M, Lopes F J S, Ramires T, Lima B R O (2012). Study of biomass emissions in the central State of São Paulo: meteorological conditions during August 2010 cause an accumulation of pollutants in the Ourinhos region. *Proceedings, XI Congresso Argentino de Meteorologia*, Mendoza, Argentina, 28 May – 01 June 2012, 8p.
- [26] Held G, Bassan J M, Frascarelli Jr R S (2011). Continuous Monitoring of the Lower Boundary Layer in the central State of São Paulo, Brazil, with a SODAR. *Geophysical Research Abstracts*, 13, EGU General Assembly 2011, Vienna, Austria, 03-08 April 2011. [http://presentations.copernicus.org/EGU2011-13634\\_presentation.pdf](http://presentations.copernicus.org/EGU2011-13634_presentation.pdf)
- [27] Feliz G S (2012). Aspectos sobre a análise meteorológica do jato de baixo nível na cidade de Bauru. Monografia para BSc (Geografia), USC, Bauru, 2012, 70p.
- [28] Karam H A (2002). Estudo do Jato de Baixo Nível de Iperó e das Implicações no Transporte de Poluentes no Estado de São Paulo. Tese de doutorado, IAG/USP, São Paulo, 2002, 213p.
- [29] Held G, Danford I R, Hong Y, Tosen G R, Preece A R (1990). *The life cycle of the low-level wind maximum in the Eastern Transvaal Highveld: A cross-sectional study*. A Report to the CSIR Executive and the Management of Eskom Engineering Investigations, CSIR Report EMA-C 90146, Pretoria, September 1990, 50p.
- [30] CETESB (2012). [http://sistemasinter.cetesb.sp.gov.br/Ar/mapa\\_qualidade/mapa\\_qualidade\\_interior.asp?id=350431](http://sistemasinter.cetesb.sp.gov.br/Ar/mapa_qualidade/mapa_qualidade_interior.asp?id=350431)
- [31] CETESB (2002). Relatório de qualidade do ar do Estado de São Paulo em 2001. CETESB, São Paulo, 132p. <http://www.cetesb.sp.gov.br/ar/qualidade-do-ar/31-publicacoes-e-relatorios>
- [32] WHO (2005). *WHO Air Quality Guidelines: Global update 2005*. Report on Working Group Meeting, Bonn/Germany, 18-20 October 2005, 30p.

- [33] Steffens J, Da Costa R F, Landulfo E, Guardani R, Moreira P F Jr, Held G (2011). Remote sensing detection of atmospheric pollutants using lidar, sodar and correlation with air quality data in an industrial area. *Proceedings, SPIE Remote Sensing Conference, Prague, Czech Republic, 19-22 September 2011*, v.8182, 81820Z; doi: 10.1117/12.897915.
- [34] Da Rocha G O, Allen A G, Cardoso A A (2004). Influence of sugar cane burning on aerosol soluble ion composition in southeastern Brazil. *Atmos. Environ.*, 38, 5025-5038.
- [35] Campos M L A M, Urban R C, Da Silva L C, Souza M L, Allen A G (2012). Use of levoglucosan, potassium, and water-soluble organic carbon to characterize the origins of biomass burning aerosols. Submitted to *Atmos. Environ.*, March 2012.
- [36] Da Rocha G O, Franco A, Allen A G, Cardoso A A (2003). Sources of atmospheric acidity in an agricultural-industrial region of São Paulo State, Brazil. *J. Geophys. Res.*, 108(D7), 1-11.
- [37] Godoi R H M, Godoi A F L, Worobiec A, Andrade S J, de Hoog J, Santiago-Silva M R, Van Grieken R (2004). Characterisation of sugar cane combustion particles in the Araraquara region, Southeast Brazil. *Microchim. Acta*, 145, 53-56.
- [38] Godoi A F L, Ravindra K, Godoi R H M, Andrade S J, Santiago-Silva M, Van Vaeck L, Van Grieken R (2004). Fast chromatographic determination of polycyclic aromatic hydrocarbons in aerosol samples from sugar cane burning. *J. Chromatog.*, A 1027, 49-53.
- [39] Kirchhoff V W J H, Marinho E V A, Dias P L S, Pereira E B, Calheiros R, André R, Volpe C (1991). Enhancements of CO and O<sub>3</sub> from burnings in sugar cane fields. *J. Atmos. Chem.*, 12, 87-102.
- [40] Oppenheimer C, Tsanev V I, Allen A G, McGonigle A J S, Cardoso A A, Wiatr A, Paterlini W, Dias C M (2004). NO<sub>2</sub> emissions from agricultural burning in São Paulo, Brazil. *Environ. Sci. Technol.*, 38, 4557-4561.
- [41] CETESB (2002). Companhia de Tecnologia de Saneamento Ambiental. Avaliação dos compostos orgânicos provenientes da queima de palha de cana-de-açúcar na região de Araraquara e comparação com medições efetuadas em São Paulo e Cubatão (relatório final – 2002). CETESB, São Paulo, 97p. <http://www.cetesb.sp.gov.br/Ar/publicacoes.asp>
- [42] Zamperlini G C M, Santiago-Silva M, Vilegas W (1997). Identification of polycyclic aromatic hydrocarbons in sugar-cane soot by gas chromatography mass spectrometry. *Chromatographia*, 46, 655-663.
- [43] Zamperlini G C M, Santiago-Silva M, Vilegas W (2000). Solid-phase extraction of sugar-cane soot extract for analysis by gas chromatography with flame ionisation and mass spectrometric detection. *J. Chromatog.*, A 889, 281-286.
- [44] De Andrade S J, Cristale J, Silva F S, Zocolo G J, Marchi M R R (2010). Contribution of sugar-cane harvesting season to atmospheric contamination by polycyclic aromatic hydrocarbons (PAHs) in Araraquara city, Southeast Brazil. *Atmos. Environ.*, 44, 2913-2919.
- [45] Cançado J E D, Saldiva P H N, Pereira L A A, Lara L B L S, Artaxo P, Martinelli LA, Arbex MA, Zanobetti A, Braga A L F (2006). The impact of sugar cane-burning emissions on the respiratory system of children and the elderly. *Environ. Hlth. Persp.*, 114, 725-729.
- [46] Miranda R M, Andrade M D, Worobiec A, Van Grieken R (2002). Characterisation of aerosol particles in the São Paulo Metropolitan Area. *Atmos. Environ.*, 36, 345-352.

- [47] Machado C M D, Cardoso A A, Allen A G (2008). Atmospheric emission of reactive nitrogen during biofuel ethanol production. *Environ. Sci. Technol.*, 42, 381-385.
- [48] Gaffney J S, Marley N A (2009). The impacts of combustion emissions on air quality and climate – From coal to biofuels and beyond. *Atmos. Environ.*, 43, 23-36.
- [49] Martins E M, Arbilla G (2003). Computer modeling study of ethanol and aldehyde reactivities in Rio de Janeiro urban air. *Atmos. Environ.*, 37, 1715-1722.
- [50] Braunbeck O, Bauen A, Rosillo-Calle F, Cortez L (1999). Prospects for green cane harvesting and cane residue use in Brazil. *Biomass Bioenergy*, 17, 495-506.
- [51] Castanho D A, Artaxo P (2001). Wintertime and summertime São Paulo aerosol source apportionment study. *Atmos. Environ.*, 35, 4889-4902.
- [52] Alonso C D, Martins M H R B, Romano J, Godinho R (1997). São Paulo aerosol characterization study. *J. Air Waste Mgt. Assoc.*, 47, 1297-1300.
- [53] Sanchez-Ccoyllo O R, Andrade M D (2002). The influence of meteorological conditions on the behavior of pollutants concentrations in São Paulo, Brazil. *Environ. Poll.*, 116, 257-263.
- [54] Miranda R M, Andrade M F (2005). Physicochemical characteristics of atmospheric aerosol during winter in the São Paulo Metropolitan area in Brazil. *Atmos. Environ.*, 39, 6188-6193.
- [55] Ynoue R Y, Andrade M D (2004). Size-resolved mass balance of aerosol particles over the São Paulo metropolitan area of Brazil. *Aerosol Sci. Technol.*, 38, 52-62.
- [56] Bourotte C, Curl-Amarante A P, Forti M C, Pereira L A A, Braga A L, Lotufo P A (2007). Association between ionic composition of fine and coarse aerosol soluble fraction and peak expiratory flow of asthmatic patients in São Paulo city (Brazil). *Atmos. Environ.*, 41, 2036-2048.
- [57] Albuquerque A T T, Andrade M F, Ynoue R Y (2012). Characterization of atmospheric aerosols in the city of São Paulo, Brazil: Comparisons between polluted and unpolluted periods. *Environ. Monit. Assess.*, 184, 969-984.
- [58] Gioda A, Sales J A, Cavalcanti P M S, Maia M F, Maia L F P G, Aquino Neto F R (2004). Evaluation of air quality in Volta Redonda, the main metallurgical industrial city in Brazil. *J. Braz. Chem. Soc.*, 14, 856-864.
- [59] Toledo V E, Almeida Júnior P B, Quiterio S L, Arbilla G, Moreira A, Escaleira V, Moreira J C (2008). Evaluation of levels, sources and distribution of toxic elements in PM<sub>10</sub> in a suburban industrial region of Rio de Janeiro, Brazil. *Environ. Monit. Assess.*, 139, 49-59.
- [60] Gioia S M C L, Babinski M, Weiss D J, Kerr A A F S (2010). Insights into the dynamics and sources of atmospheric lead and particulate matter in São Paulo, Brazil, from high temporal resolution sampling. *Atmos. Res.*, 98, 478-485.
- [61] Miranda R, Tornaz E (2008). Characterization of urban aerosol in Campinas, São Paulo, Brazil. *Atmos. Res.*, 87, 147-157.
- [62] Sanchez-Ccoyllo O R, Silva Dias P L, Andrade M D, Freitas S R (2006). Determination of O<sub>3</sub>, CO, and PM<sub>10</sub> transport in the metropolitan area of São Paulo, Brazil through synoptic-scale analysis of back trajectories. *Meteorol. Atmos. Phys.*, 92, 83-93.
- [63] Allen A G, Miguel A H (1995). Indoor organic and inorganic pollutants - In-situ formation and dry deposition in southeastern Brazil. *Atmos. Environ.*, 29, 3519-3526.

- [64] Vasconcellos P C, Souza D Z, Magalhaes D, Da Rocha G O (2011). Seasonal variation of n-alkanes and polycyclic aromatic hydrocarbon concentrations in PM<sub>10</sub> samples collected at urban sites of São Paulo State, Brazil. *Water Air Soil Poll.*, 222, 325-336.
- [65] Vasconcellos P C, Souza D Z, Avila S G, Araujo M P, Naoto E, Nascimento K H, Cavalcante F S, Dos Santos M, Smichowski P, Behrentz E (2011). Comparative study of the atmospheric chemical composition of three South American cities. *Atmos. Environ.*, 45, 5770-5777.
- [66] Bourotte C, Forti M C, Taniguchi S, Bicego M C, Lotufo P A (2005). A wintertime study of PAHs in fine and coarse aerosols in São Paulo city, Brazil. *Atmos. Environ.*, 39, 3799-3811.
- [67] Allen A G, McGonigle A J S, Cardoso A A, Machado C M D, Davison B, Paterlini W, Da Rocha G O, De Andrade J B (2009). Influence of sources and meteorology on surface concentrations of gases and aerosols in a coastal industrial complex. *J. Braz. Chem. Soc.*, 20, 214-221.
- [68] Vautz W, Pahl S, Pilger H, Schilling M, Klockow D (2003). Deposition of trace substances via cloud droplets in the Atlantic rain forest of the Serra do Mar, São Paulo State, SE Brazil. *Atmos. Environ.*, 37, 3277-3287.
- [69] Allen A G, Da Rocha G O, Cardoso A A, Paterlini W C, Machado C M D (2008). Atmospheric particulate polycyclic aromatic hydrocarbons from road transport in southeast Brazil. *Transportation Res.*, 13, 483-490.
- [70] Bourotte C, Forti M C, Melfi A J, Lucas Y (2006). Morphology and solutes content of atmospheric particles in an urban and a natural area of São Paulo State, Brazil. *Water Air Soil Poll.*, 170, 301-316.
- [71] Vasconcellos P C, Souza D Z, Sanchez-Ccoyllo O, Bustillos J O V, Lee H, Santos F C, Nascimento K H, Araujo M P, Saarnio K, Teinila K, Hillamo R (2010). Determination of anthropogenic and biogenic compounds in atmospheric aerosol collected in urban, biomass burning and forest areas in São Paulo, Brazil. *Sci. Tot. Environ.*, 408, 5836-5844.
- [72] Landulfo E, Papayannis A, Artaxo P, Castanho A D A, Freitas A Z, De Souza R F, Junior N D V, Jorge M, Sánchez-Ccoyllo O R, Moreira D S (2003). Synergetic measurements of aerosols over São Paulo, Brazil using lidar, sunphotometer and satellite data during the dry season. *Atmos. Chem. Phys.*, 3, 1523-1539; doi:10.5194/acp-3-1523-2003.
- [73] Da Costa R F (2010). Study of the optical properties of aerosols in the State of São Paulo with the Raman Lidar technique. Master Dissertation, Centro de Lasers e Aplicações, Instituto de Pesquisas Energéticas e Nucleares, Universidade de São Paulo, São Paulo, Brazil, 90p.
- [74] Torres A S (2008). Development of a methodology for an independent water vapor Raman Lidar calibration to study water vapor atmospheric profiles, PhD Thesis, Centro de Lasers e Aplicações, Instituto de Pesquisas Energéticas e Nucleares, Universidade de São Paulo, São Paulo, Brazil, 144p.
- [75] Lopes F J S (2011). Validation of elastic backscatter lidar data from the CALIPSO satellite using the AERONET sun photometer network. PhD thesis, Centro de Lasers e Aplicações, Instituto de Pesquisas Energéticas e Nucleares, Universidade de São Paulo, São Paulo, Brazil, 169p.

- [76] Larroza E G (2011). Caracterização das Nuvens Cirrus na Região Metropolitana de São Paulo (RMSP) com a Técnica de Lidar de Retroespalhamento Elástico. PhD thesis, Centro de Lasers e Aplicações, Instituto de Pesquisas Energéticas e Nucleares, Universidade de São Paulo, São Paulo, Brazil, 118p.
- [77] Landulfo E, Held G, De Freitas A Z, Papayannis A, De Souza A F (2007). Results from first lidar measurements in the central State of São Paulo during the TroCCiBras 2004 Campaign with IPEN'S aerosol lidar. *Abstracts, 4th Workshop on Lidar Measurements in Latin America*, Ilhabela, S.P., 17-22 June 2007. [http://www.ipen.br/sitio/LWS\\_Brasil/p4w\\_abstracts.htm](http://www.ipen.br/sitio/LWS_Brasil/p4w_abstracts.htm)
- [78] Held G, Pommereau J-P, Schumann U (2008). TroCCiBras and its partner projects HIBISCUS and TROCCINOX: The 2004 Field Campaign in the State of São Paulo. *Opt.Pura. Apl.*, 41 (2), 207-216. [http://www.sedoptica.es/Menu\\_Volumenes/pdfs/299.pdf](http://www.sedoptica.es/Menu_Volumenes/pdfs/299.pdf)
- [79] Landulfo E, Lopes F J S, Mariano G L, Torres A S, Jesus W C, Nakaema W M, Jorge M, Mariani R (2010). Study of the properties of aerosols and the air quality index using a backscatter lidar system and AERONET sunphotometer in the city of São Paulo, Brazil. *J. Air Waste Manage. Assoc.*, 60, 386–392; doi: 10.3155/1047-3289.60.4.386.
- [80] Landulfo E, Lopes F J S (2009). Initial approach in biomass burning aerosol transport tracking with Calipso and Modis satellites, sunphotometer and a backscatter lidar system in Brazil. *Proceedings of SPIE – The International Society for Optical Engineering*, Vol. 7479, 747905, 2009; doi: 10.1117/12.829973.
- [81] Stohl A (1999). *The FLEXTRA Trajectory Model, Version 3.0: User Guide*. Lehrstuhl für Bioklimatologie und Immissionsforschung, University of Munich, Freising, Germany, 1999, 41p. Available from: <http://www.forst.uni-muenchen.de/LST/METEOR/stohl/flextra.htm>
- [82] Lopes F J S, Landulfo E, Giannakaki E (2008). One-Year of CALIPSO Measurements Over the City of São Paulo, In: *Reviewed and Revised Papers presented at the 24<sup>th</sup> International Laser Radar Conference 2008*, Boulder, Colorado, v. 2, 1169-1172.
- [83] Landulfo E, Jorge M P, Held G, Guardani R, Steffens J, Pinto S A F, Andre I R, Garcia A G, Lopes F J S, Mariano G L, Da Costa R F, Rodrigues P F (2010). Lidar observation campaign of sugar cane fires and industrial emissions in the State of São Paulo, Brazil. *SPIE Digital Library, Proc. SPIE*, Vol. 7832, 783201 (2010), 8p; doi: 10.1117/12.866078.
- [84] Mariano G L, Lopes F J S, Steffens J, Jorge M P P M, Landulfo E, Held G, Pinto S A F (2011). Aerosols monitoring in Rio Claro, Brazil, using LIDAR and air pollution analyzers. *Opt. Pura Apl.*, 44, 55-64.
- [85] Held G, Lopes F J S, Bassan J M, Nery J T, Cardoso A A, Gomes A M, Ramires T, Lima B R O, Allen A G, Da Silva L C, Souza M L, De Souza K F, Carvalho L R F, Urban R C, Landulfo E, Decco A M, Campos M L A A, Nassur M E Q, Nogueira R F P (2011). Raman lidar monitors emissions from sugar cane fires in the State of São Paulo: A pilot project integrating radar, sodar, aerosol and gas observations. *Revista Boliviana de Física*, 20, 24-26. [Full paper submitted to *Opt. Pura Apl.* in February 2012].
- [86] Held G, Larroza E G, Lopes F J S, Da Costa R F, Landulfo E (2011). Raman lidar and sodar measurements in the State of São Paulo, Brazil. *Proceedings, 2011 NDACC Symposium*, Reunion Island, 07-10 November 2011, 4p.

- [87] Lopes F J S, Held G, Nakaema W M, Rodrigues P F, Bassan J M, Landulfo E (2011). Initial analysis from a lidar observation campaign of sugar cane fires in the central and western portion of the São Paulo State, Brazil In: Lidar Technologies, Techniques, and Measurements for Atmospheric Remote Sensing VII, 2011. Czech Republic: *Proceedings of SPIE - The International Society for Optical Engineering*, vol. 8182, 818214; doi: 10.1117/12.898119.
- [88] Steffens J, Guardani R, Landulfo E, Lopes F J S, Moreira P F, Moreira A (2011). Capability of atmospheric air monitoring in the urban area of Cubatão using lidar technique. *Opt. Pura Apl.*, 44, 65-70.
- [89] Dixon M, Wiener G (1993). TITAN: Thunderstorm Identification, Tracking, Analysis & Nowcasting - A radar-based methodology, *J. Atmos. Oceanic Technol.*, 10, 785-797.
- [90] Cattrall C, Reagan J, Thome K, Dubovik O (2005). Variability of aerosol and spectral lidar and backscatter and extinction ratios of key aerosol types derived from selected Aerosol Robotic Network locations, *Journal of Geophysical Research*, 110, D10S11. doi:10.1029/2004JD005124.
- [91] Omar A H, Winker D M, Kittaka C, Vaughan M A, Liu Z, Hu Y, Trepte C R, Rogers R R, Ferrare R A, Lee K P, Kuehn R E, Hostetler C A (2009). The CALIPSO Automated Aerosol Classification and Lidar Ratio Selection Algorithm, *Journal of Atmospheric and Oceanic Technology*, 26, 1994-2014; doi:10.1175/2009JTECHA1231.1.
- [92] Da Silva L C, Allen A G, Cardoso A A, Held G (2011). Aerosol physical and chemical characteristics in the region of Ourinhos (São Paulo State). *Proceedings, Second Conference of the Brazilian Association for Aerosol Research*, Rio de Janeiro, 1-5 August 2011.
- [93] De Oliveira B F A, Ignotti E, Hacon S S (2011). A systematic review of the physical and chemical characteristics of pollutants from biomass burning and combustion of fossil fuels and health effects in Brazil. *Cadernos de Saúde Pública*, 27, 1678-1698.
- [94] Castro H A D, Cunha M F D, Mendonça G A S, Junger W L, Cunha-Cruz J, Ponce de Leon A (2009). Effect of air pollution on lung function in schoolchildren in Rio de Janeiro, Brazil. *Rev. Saúde Pública*, 43, 26-34.
- [95] CETESB (2008). Companhia de Tecnologia de Saneamento Ambiental. Relatório de qualidade do ar no estado de São Paulo 2007. CETESB, São Paulo. <http://www.cetesb.sp.gov.br/Ar/publicacoes.asp>
- [96] Gouveia N, Freitas C U, Martins L C, Marcilio I O (2006). Hospitalizações por causas respiratórias e cardiovasculares associadas à contaminação atmosférica no Município de São Paulo, Brasil. *Cad. Saúde Pública*, 22, 2669-2677.
- [97] Braga A L, Saldiva P H, Pereira L A, Menezes J J, Conceição G M, Lin C A, Zanobetti A, Schwartz J, Dockery D W (2001). Health effects of air pollution exposure on children and adolescents in São Paulo, Brazil. *Pediatr. Pulmonol.*, 31, 106-13.
- [98] Conceição G M S, Miraglia S G E K, Kishi H S, Saldiva P H N, Singer J M (2001). Air pollution and child mortality: a time-series study in São Paulo, Brazil. *Environ. Hlth. Persp.*, 109, 347-350.
- [99] Gouveia N, Fletcher T (2000). Respiratory disease in children and outdoor air pollution in São Paulo, Brazil: a time-series analysis. *Occup. Environ. Med.*, 57, 477-483.
- [100] Martins L C, Latorre M R D O, Saldiva P H N, Braga A L F (2001). Relação entre poluição atmosférica e atendimentos por infecção das vias aéreas superiores no

- município de São Paulo: avaliação do rodízio de veículos. *Rev. Brás. Epidemiol.*, 4, 220-229.
- [101] Martins L C, Latorre M R D O, Saldiva P H, Braga A L (2002). Air pollution and emergency room visits due to chronic lower respiratory disease in the elderly: an ecological times-series study in São Paulo, Brazil. *J. Occup. Environ. Med.*, 44, 622-627.
- [102] Miraglia S G E K, Saldiva P H N, Böhm G M (2005). An evaluation of air pollution health impacts and costs in São Paulo, Brazil. *Environ. Mgt.*, 35, 667-676.
- [103] Gouveia N, Mendonça G A S, Ponce de Leon A, Correia J E M, Junger W L, Freitas C U, Daumas R P, Martins L C, Guissepe L, Conceição G M S, Manerich A, Cunha-Cruz J (2003). Poluição do ar e efeitos na saúde nas populações de duas grandes metrópoles brasileiras. *Epidemiol. Serv. Saúde*, 12, 29-40.
- [104] Freitas C, Bremner S A, Gouveia N, Pereira L A, Saldiva P H N (2004). Internações e óbitos e sua relação com a poluição atmosférica em São Paulo, 1993 a 1997. *Rev. Saúde Pública*, 38, 751-757.
- [105] Martins M C H, Fatigati F L, Véspoli T C, Martins L C, Pereira L A A, Martins M A, Saldiva P H N, Braga A L F (2004). Influence of socioeconomic conditions on air pollution adverse health effects in elderly people: an analysis of six regions in São Paulo, Brazil. *J. Epidemiol. Community Health*, 58, 41-46.
- [106] Spektor D M, Hofmeister V A, Artaxo P, Brague J A P, Echelar F, Nogueira D P, Hayes C, Thurston G D, Lippmann M (1991). Effects of heavy industrial pollution on respiratory function in the children of Cubatão, Brazil - A preliminary report. *Environ. Hlth. Persp.*, 94, 51-54.
- [107] De Martinis B S, Kado N Y, Carvalho L R F, Okamoto R A, Gundel L A (1999). Genotoxicity of fractionated organic material in airborne particles from São Paulo, Brazil. *Mutation Res.*, 446, 83-94.
- [108] De Martinis B S, Okamoto R A, Kado N Y, Gundel L A, Carvalho L R F (2002). Polycyclic aromatic hydrocarbons in a bioassay-fractionated extract of PM<sub>10</sub> collected in São Paulo, Brazil. *Atmos. Environ.*, 36, 307-314.
- [109] Vasconcellos P C, Sanchez-Ccoyllo O, Balducci C, Mabilia R, Cecinato A, (2008). Occurrence and concentration levels of nitro-PAH in the air of three Brazilian cities experiencing different emission impacts. *Water Air Soil Poll.*, 190, 87-94.
- [110] Vendrasco E P, Silva Dias P L, Freitas E D (2009). A case study of the direct radiative effect of biomass burning aerosols on precipitation in the Eastern Amazon. *Atmos. Res.*, 94, 409-421.
- [111] Martins J A, Silva Dias M A F (2009). The impact of smoke from forest fires on the spectral dispersion of cloud droplet size distributions in the Amazonian region. *Env. Res. Lett.*, 4, art. no. 015002.
- [112] Moreira J R, Goldemberg J (1999). The Alcohol Program. *Energy Policy*, 27, 229-245.
- [113] Arbex M A, Böhm G M, Saldiva P H N, Conceição G M S, Pope III A C, Braga A L F (2000). Assessment of the effects of sugar cane plantation burning on daily counts of inhalation therapy. *J. Air Waste Mgt. Assoc.*, 50, 1745-1749.
- [114] Arbex M A, Martins L C, Oliveira R C, Pereira L A, Arbex F F, Cançado J E, Saldiva P H, Braga A L (2007). Air pollution from biomass burning and asthma hospital



- admissions in a sugarcane plantation area in Brazil. *J. Epidemiol. Comm. Hlth.*, 61, 395-400.
- [115] Lopes F S, Ribeiro H (2006). Mapeamento de internações hospitalares por problemas respiratórios e possíveis associações à exposição humana aos produtos da queima de palha de cana-de-açúcar no estado de São Paulo. *Rev. Brás. Epidemiol.*, 9, 215-225.
- [116] Mazzoli-Rocha F, Magalhães C B, Malm O, Saldiva P H, Zin W A, Faffe D S (2008). Comparative respiratory toxicity of particles produced by traffic and sugarcane burning. *Environ. Res.*, 108, 35-41.
- [117] De Andrade S J, Varella S D, Pereira G T, Zocolo G J, De Marchi M R R, Varanda E A (2011). Mutagenic activity of airborne particulate matter (PM<sub>10</sub>) in a sugarcane farming area (Araraquara city, southeast Brazil). *Environ. Res.*, 111, 545-550.
- [118] Bell T L, Rosenfeld D, Kim K M, Yoo J M, Lee M I, Hahnenberger M (2008). Midweek increase in US summer rain and storm heights suggests air pollution invigorates rainstorms. *J. Geophys. Res.*, 113, D2, Art. No. D02209.
- [119] IPCC (2007). Fourth Assessment Report "Climate Change 2007", International Panel on Climate Change: [www.ipcc.ch](http://www.ipcc.ch).
- [120] Rosenfeld D (2006). Aerosol-cloud interactions control of earth radiation and latent heat release budgets. *Space Sci. Rev.*, 125, 149-157.
- [121] Dufek A S, Ambrizzi T (2008). Precipitation variability in São Paulo State, Brazil. *Theoret. Appl. Climatol.*, 93, 167-178.
- [122] Coelho C H, Allen A G, Fornaro A, Orlando E A, Grigoletto T L B, Campos M L A M (2011). Wet deposition of major ions in a rural area impacted by biomass burning emissions. *Atmos. Environ.*, 45, 5260-5265.
- [123] UNICA (2012). <http://english.unica.com.br/dadosCotacao/estatistica/> (Accessed 29/4/2012).
- [124] Gomes A M, Escobedo J F (2010). Climatologia de Tempestades na Área Central do Estado de São Paulo Usando Radar Meteorológico. *Revista Energia na Agricultura*, 25, no. 1, 1-20. ISSN- 1808-875.
- [125] Westcott N E (1995). Summertime cloud-to-ground lightning activity around major Midwestern urban areas. *J. Appl. Meteor.*, 34, 1633-1642.
- [126] UNICA (2011). (Accessed 17/4/2012) <http://english.unica.com.br/website/userFiles/protocolo-agroambiental.pdf>
- [127] Tsao C C, Campbell J E, Mena-Carrasco M, Spak S N, Carmichael G R, Chen Y (2012). Increased estimates of air-pollution emissions from Brazilian sugar-cane ethanol. *Nature Climate Change*, 2, 53-57.